Delft University of Technology
Master's Thesis in Embedded Systems

Crowd Distribution Estimation using Smart Lighting Grids

Renukaprasad Manjappa

PHILIPS
Lighting

embedded
software

TU Delft Delft University of Technology

Crowd Distribution Estimation using Smart Lighting Grids

Master's Thesis in Embedded Systems

Embedded Software Section
Faculty of Electrical Engineering, Mathematics and Computer Science
Delft University of Technology
Mekelweg 4, 2628 CD Delft, The Netherlands

Renukaprasad Manjappa
r.b.manjappa@student.tudelft.nl

November 21, 2017

Author
Renukaprasad Manjappa (r.b.manjappa@student.tudelft.nl)
Title
Crowd Distribution Estimation using Smart Lighting Grids
MSc presentation
November 21, 2017

Graduation Committee

Prof. dr. Koen Langendoen	Delft University of Technology
Dr. R. Venkatesha Prasad	Delft University of Technology
Dr. ir. Vijay. S. Rao	Delft University of Technology
Dr. ir. Arjan van Genderen	Delft University of Technology
Mr. Peter Krom	Philips Lighting Research, Eindhoven

Abstract

Estimating the number of people in a given area and knowing their positions open up numerous possibilities for a variety of smart data driven applications. Most of the existing systems either require active participation from people in the crowd or are too expensive to be deployed. The exponentially increasing adoption of smartphones by people and the ubiquitous Wi-Fi infrastructure motivated us to tackle this problem in a non-intrusive manner.

This thesis focuses on designing a system to infer the crowd distribution in large indoor spaces. As we choose to be non-intrusive in approach, we incorporate low cost Wi-Fi sniffers into smart bulbs that are part of the lighting grids in buildings. The Wi-Fi data gathered from these smart bulbs is analyzed to obtain people count and the people's position within a given area. Our aim is to estimate people's location within 4x4 m^2 grids with minimal number of Wi-Fi frames.

A number of filtering and post processing mechanisms are proposed in order to eliminate false positives and to accurately identify the number of people within a given area. Extensive experiments are conducted in a real-world testbed with controlled settings as well as in test setups with no control (auditorium and a coffee corner). The improvised counting algorithm comes close to 75% of the ground truth.

We adopt range free localization algorithms to estimate the position of people and evaluate these algorithms extensively. We propose enhancements on these algorithms to refine the position estimation accuracy and reduce the execution time. Range free localization algorithms were able to estimate the position 40% of the time within 2m when sniffers are placed 6m apart in a grid topology in a highly multipath testbed environment. Simulations indicate this number can increase up to 76% when sniffers are placed 4m for the same topology.

Since the bulbs with sniffers cost more we minimize the overall deployment cost of the system by reducing the number of sniffers while maintaining an accuracy within a 4x4 m^2 grid majority of the time. Extensive simulations are run with different topologies and sniffer densities in order to find this sweet spot.

"The hardest thing of all is to find a black cat in a dark room, especially if there is no cat" –Confucius

Preface

The potential applications of sniffing Wi-Fi channels non-intrusively had captivated my interests ever since I tried it for the first time. The idea that a plethora of information was so easily available in the air for anyone who wishes tap into it fascinated me. The project was appealing to me as it gave me an opportunity to deduce how this information can be linked to various activities such as Crowd distribution or Social interactions just by sniffing the Wi-Fi channels.

I would like to thank my supervisors Dr. Rangarao Venkatesha Prasad and Dr. Vijay S Rao for their continuous guidance and support throughout the tenure of my thesis. Their encouragement and kind words of wisdom has always inspired me to put forward my best work.

I extend my sincere gratitude to my mentors Peter Krom, Alexandre Sinitsyn and Bram Joosen at Philips Lighting Research, Eindhoven for providing an excellent platform to pursue my research activities. I would like to thank the entire Systems team including Olaf, Rian, Chandra, Nick and Kevin for their suggestions whenever I felt stuck. Special thanks to Alex Palaios for sharing his insights with respect to radio propagation anomalies.

I would also like to thank my parents and my sister without whose belief and support I could not have pursued my dreams. A final shout out to two of my best friends Shruthi and Sumanth for keeping me sane throughout this roller coaster ride.

Renukaprasad Bankasanada Manjappa

Delft, The Netherlands
November 14, 2017

Contents

Chapter 1

Introduction

Crowd density (or distribution) estimation is an important parameter for various smart applications in the connected world. Crowd distribution estimation involves finding the number of people and their approximate location within a given area. This information opens up possibilities for various location based services. It has use cases in many areas including business intelligence, surveillance, crowd management, intelligent environments and smart cities of the future. In retail environment we can utilize this information to improve shopping experience, increase the sales, or to evaluate the performance of products vis--vis their sales. In crowd management, crowd behaviour can be monitored to avoid unpleasant incidents such as the 2010 Love Parade disaster in Germany, where 21 people died and more than 500 were injured. In smart city applications, crowd distribution information can be used to optimize resource usage, e.g., scheduling of the transportation system depending on the density of the crowd. Furthermore, information about the crowd and people movement in indoors can be utilized to improve energy efficiency of the building by optimizing heating and lighting, or to develop emergency evacuation strategies.

A comprehensive survey by Teixeira et al. [36] indicates that future human sensing systems are more likely to be consisting of either a large number of low-cost sensors, mobile phone sensors and a less number of cameras that are placed in key locations. The problem of estimating crowd distribution has been previously tackled using either sophisticated image processing based approaches which are expensive to deploy when the area is large or require participation from people in the crowd.

The ever-increasing ubiquitous Wi-Fi infrastructure and the increasing adoption of smartphones by people motivated us to design a non-intrusive system that can infer crowd distribution by tracking smartphones that people carry with them. The main assumption is that most of the people carry smartphones with them and have their Wi-Fi switched ON irrespective of being connected to a network. By finding the number of users connected to

the WiFi access point could indirectly reveal the number of people present. However, smartphones are not always connected and WiFi in some mobiles may be OFF. Not all in the crowd may carry a smartphone too. Now with those mobiles switched ON if we can sniff WiFi signals an estimation could be made as to how many persons are in a given area. However, there are many challenges to realize this. In the sequel below we briefly discuss our approach and formulate the problem tackled in this thesis.

Further, majority of the previous works involving passive Wi-Fi sniffing do not provide fine grained position estimates. The granularity is either campus wide deployments or within the sensing range of a single sniffer. This introduces ambiguity into the system as a person can be present anywhere within hundreds of meters. The ambiguity in position makes it difficult to develop smart applications.

In the meantime, there is much development in the indoor lighting domain. The advent of LED bulbs has bridged the ICT domain with the lighting systems. Many sensors could be housed into the LED bulbs because of the advancements in microelectronics. Thus our approach is to incorporate Wi-Fi sniffers into smart light bulbs as part of the smart lighting grid of a building such as an arena concourse or auditorium in order to estimate the crowd distribution within a bounded area. Each light bulb sniffs for Wi-Fi signals in its vicinity. The data from a number of such sniffer bulbs is combined to estimate the overall crowd distribution of the area.

Figure 1.1: Concept of Smart bulbs with built in sniffing ability.

1.1 Problem Statement

Majority of the work related to estimating the crowd distribution either requires expensive hardware or participation from people in the crowd to obtain accurate results. The Approaches involving Non-intrusive Wi-Fi sniffing have mainly focused on providing rough estimates of people count without any form of filtering. The granularity of position estimation has also been

quite large ranging from city wide to campus wide deployments.

In our approach we are specifically interested in knowing the distribution of people in the crowd within a bounded indoor space based on the Wi-Fi sniffing data obtained from smart light bulbs. This involves design of a system that can infer people count as well as their position within the given area. As the Wi-Fi sniffers will be part of lighting grids of the indoor space, several constraints are imposed on the system. They are listed below:

- Due to passive nature of Wi-Fi sniffing the number of packets received and the frequency at which packets arrive may not be consistent over time and with respect to number of devices sniffed.
- As we wish to be non-intrusive we do not attempt to increase packet generation rate from smartphones by injecting packets into the network.
- Due to increase in the number of devices with Wi-Fi interface considerable errors will be introduced if we use the sniffed data directly without any form of filtering.
- Position estimation can be a challenging due several unknowns in the system such as unknown TX power, orientation and antenna characteristics, which are not in our control.

Given these constraints imposed on the system, we address the following problems to realize ***accurate*** **density estimation**.

- How to estimate the number of people in a given area solely based on Wi-Fi sniffing data obtained from smart bulbs?
- How to efficiently filter unwanted devices encountered during sniffing to refine the count?
- How to estimate the position of a user with an accuracy of a 4mx4m grid with minimal number of samples?
- How to minimize the deployment cost of by reducing the number of sniffers while maintaining an acceptable localization accuracy?

The answers to these important questions helps in realizing our goal. we address them in the further chapters.

1.2 Contributions

The thesis proposes a system to infer crowd distribution for a given area. The main contributions are summarized as follows :

- We provide a thorough analysis of Wi-Fi signals from a smartphone in order to understand various parameters such as assortment of Wi-Fi packet types, inter packet interval under different smartphone configurations.
- we propose an improved people counting algorithm with efficient filtering mechanisms to estimate people count within a given area.
- We undertake an extensive evaluation of localization algorithms to estimate and improve the position estimation.
- We also look into different sniffer deployment topologies and densities in order to minimize the deployment cost while maintaining a reasonable localization accuracy.
- We propose a mechanism to assess the reliability of position estimation using confidence scores.

1.3 Thesis Organization

Chapter 2 gives a brief description of the related work and classification of different approaches used to deduce crowd density. Chapter 3 gives information regarding the system architecture and the general challenges that need to be addressed. It also provides an overview of 802.11 packet sniffing and an analysis of time interval between packets under different smartphone configurations. Chapter 4 addresses the problem of people counting. It describes filtering and post processing mechanisms to efficiently count the number of people within a given area. It showcases the results obtained from experiments and the limitations of the approach. Chapter 5 describes localization algorithms used to estimate the position of smartphones. It provides a comparison of localization algorithms with respect to various parameters and proposes methods to refine position estimation accuracy. Chapter 6 provides insights into optimal grid configuration. Chapter 7 summarizes the conclusion from the studies and suggests some points for future work.

Chapter 2

Related Work

This chapter summarizes prior work in the area of crowd distribution analysis. Section 2.1 provides an overview of participatory techniques involving use of wearables and smartphone applications. Section 2.2 describes different techniques which do not require any participation from people in the crowd.

2.1 Participatory Techniques

These techniques require co-operation from people in the crowd in order to estimate the number of people in a given area. The participation can be in the form of wearing devices or installing a third-party application that allows them to be tracked.

2.1.1 Wearables

These techniques involve use of the wearable sensors to track people in the crowd. The sensors collect movement data using various sensors to be analyzed later. Acer et al. [3] use battery powered wearable Wi-Fi badges and a set of Wi-Fi gateways deployed at various points across the location to capture signals from the badges. Note that the badges are distributed to a select set of the participants. Having a programmable Wi-Fi badge allows efficient detection as packets are sent at a constant rate. However, this work only shows peaks and approximate number of people present, and does not show either the right density or the location of people.

Several studies of crowd dynamics at large religious gatherings have been carried out by Yamin et al. [46] [45] and Jamil et al. [25]. Yamin et al. [45] use bracelets equipped with RFID tags. Several RFID readers are installed at different sections in the area to analyze movement patterns of the crowd. Jamil et al. [25] use Bluetooth Low Energy tags and smartphones at the Hajj gathering. The authors of [45] and [46] do not demonstrate any quan-

tifiable results to showcase the count of people but only showcase the crowd movement patterns.

Cattani et al. [11] uses bracelets that emit RF beacons to estimate crowd dynamics at the Nemo Science museum in Amsterdam. Compared to previous works in this section an innovative approach is taken by the authors where neighbourhood estimation is used to calculate the crowd density in an energy-efficient manner. These methods prove to be much better in analyzing the crowd behavior in the museum. The main drawback of this method is that it requires participation from people to be effective. Providing wearables to a large crowd can significantly impact the infrastructure cost.

2.1.2 Smartphone Application

A second participatory technique is to use smartphone applications or modified network stacks on smartphones that enable tracking of the users.

The authors of [41] make use of GPS equipped smartphones to infer crowd density information. In this system, pedestrians in the crowd share their location information voluntarily. Since only a fraction of the people in the crowd may share their location information, the crowd density is analyzed based on the walking speed of the pedestrians. It is assumed that the movement speed of pedestrians is proportional to the crowd buildup in a given area. This approach is suitable for large open spaces where GPS is available. If the gathering of people is relatively small such as an Auditorium where crowds might hardly move or a museum that may have multiple floors, this solution does not perform well.

The authors of [39] use smartphones with Bluetooth interface to infer the crowd density information. The approach involves performing Bluetooth scan to discover nearby devices. It also takes into account the average signal strength and the RSSI variance to avoid static devices in the area. It has been shown in [2] that number of people who have their Bluetooth switched ON is significantly less compared to Wi-Fi. In older Android and iOS stacks, Bluetooth was by default in discoverable mode but in the latest software stacks, this feature has been removed. Thus smartphones are not discoverable by default. This can be considered as the main drawback of any Bluetooth based approach involving a smartphone including [39, 29].

Herrera et al. [20] use sound to estimate the location of an arbitrary number of co-located devices in a 3D space. The method is demonstrated to be very effective and provides sub meter level positioning. The estimation technique suffers in noisy environments and requires people to install a specific application on their smartphone.

2.2 Non-Participatory Techniques

These techniques do not require any form of co-operation from people in the crowd. Data is collected in a non-intrusive manner. This section provides a brief overview of the different technologies that have been developed to infer the crowd density using non-participatory approaches.

2.2.1 Visual Techniques

These techniques make use of various image processing and computer vision algorithms to count people in still images or live video streams. One of the most common types of approaches used is to first identify an individual in a crowded scene and then feed this data to various classifiers to get the people count. Some of the popular works with this approach is by Zhao et al. [51], Rittscher et al. [33], Cipolla et al. [9] and Tao et al. [35]. Vision based techniques perform well as long as the features can be detected effectively. People counting can also be implemented using stereo cameras that can perceive depth information as shown by Zhang et al. [50] and Dan et al. [14]. These make use of ceiling mounted depth cameras such as Kinect sensors that can detect head and shoulders for people counting.

Image processing based algorithms have several drawbacks. They suffer under severe occlusion in the crowd and poor lighting conditions. These make it difficult to detect the individual features. Furthermore, these algorithms can be used in only a line-of-sight environment. The use of cameras also raise privacy concerns. Vision based systems are known to increase the deployment costs and computational complexity of the system.

2.2.2 Wi-Fi CSI

Channel State Information (CSI) represents a fine-grained value derived from the 802.11 physical layer. CSI describes how a transmitted signal gets attenuated in the wireless channel before reaching the receiver. CSI exposes a set of channel measurements providing the amplitudes and phases of the signals. One of the most fascinating works with this approach is done by Katabi et al. [4] titled "See through walls with Wi-Fi!". It can count the number of people in a closed room and estimate their relative locations using the CSI information. This work forms the basis for crowd counting by leveraging the CSI information.

Xi et al. [42] have used CSI based approach to estimate the people count in a given area. They propose that CSI is highly sensitive to the environmental variations that might occur due to the presence of people in an area. A relationship is established between the number of moving people in an area and the CSI variations. Domenico et al. [16] also use a CSI based crowd counting system that analyzes Doppler spectrum obtained through

the gathered CSI data.

Wi-Fi CSI based techniques are device free and does not require the users to even carry smartphones with them. However, the CSI information is not easily exposed on all the Wi-Fi chipsets. Currently, only a select few variants of Atheros and Intel 5300 chips can expose the CSI information. These chips require modification of the underlying software stack [18]. Hence CSI based systems cannot be deployed on off the shelf Wi-Fi chips. This can be seen as one of the main drawbacks of such an approach.

2.2.3 Passive Wi-Fi Sniffing

These techniques make use of passive Wi-Fi scanning to infer the occupancy estimatation at a given location. This typically involves deploying Wi-Fi scanners in the area of interest to capture signals from smartphones that people might be carrying with them. Scanning is done in a non-intrusive manner without the need to modify any software or install any application on the smartphone. Bonne et al. [7] present a method for tracking people at mass events without the need for their cooperation. Hande et al. [19] proposed a system to estimate number of passengers in a public transportation system. Wang et al. [38] use similar approach to study queue time measurement using a single-point Wi-Fi monitor. Bayesian networks are used to infer service time within a 10 second resolution. Musa et al. [28] reported pedestrian tracking method using Wi-Fi monitor to collect Wi-Fi packets from smartphone. Viterbi algorithm was applied for estimating pedestrian trajectory.

Wi-Fi sniffing can also provide some additional data about the crowd along with the location analytics information. Barbara et al. [5] conducted 3 month long experiments and collected data from over 160K different devices. It has been shown how we can learn about important sociological aspects such as language, vendor adoption, and so on. Cunche et al. [13] showed that SSIDs obtained by scanning Wi-Fi packets can be used to infer social links between people in the crowd. Cheng et al. [12] extended this approach by including physical proximity and spatio-temporal behaviour.

2.2.4 Device free passive

RF based Device free passive (Dfp) techniques have the ability to localize individuals and does not require them to carry any radio devices with them. These techniques take into account how people disturb the pattern of radio waves in the area of interest and derives their location. Device free passive techniques can be further classified into Fingerprinting based and Link quality based techniques. Fingerprinting based methods involve construction of a Radio map of the environment based on training data. This method was investigated in [44, 49, 43]. Youssef et al. [49] was one of the

first who attempted to create a Radio map of the environment by placing an individual in a set of predetermined locations. The individual is then mapped to one of the locations in a probabilistic way based on the observed signal strengths. Xu et al. [44] have proposed a cell based calibration with random walk technique to improve the accuracy and reduce the calibration overhead. Fingerprinting based techniques can deal with the multipath effect of signals as it measures the ground truth at various positions. The disadvantage of this technique is the tedious training time that is required in a multi person environment.

Link-based DfP schemes attempt to capture the relationship between the radio signal strength (RSS) of a link and whether the subject is on the Line-of-Sight (LoS) of the radio link and consequently determine the subject's location. This technique was used by Wilson et al. [40] who proposed a Radio Tomographic Imaging (RTI) which aims at localizing multiple individuals relative to radio links LoS. Depatla et al. [15] try to count the number of people solely by measuring signal strength variation between a pair of stationary transmitter/ receiver antennas. They propose that people walking affect the transmitted signal either blocking the line of sight (LOS) path or scattering the signal. They establish a mathematical relationship to to express this as function of number of people in the area. Similar approach has been used by Doong et al [17] which uses not only RSSI variation but Fourier spectral features and machine learning algorithms to predict people count. Link quality based approaches require a TX-RX pair to be placed in LOS in the counting area such as corners of the room. The solution might be difficult to deploy if the counting area is quite large. The performance may reduce at larger crowd densities or if multiple targets are located very close to each other.

2.3 Summary

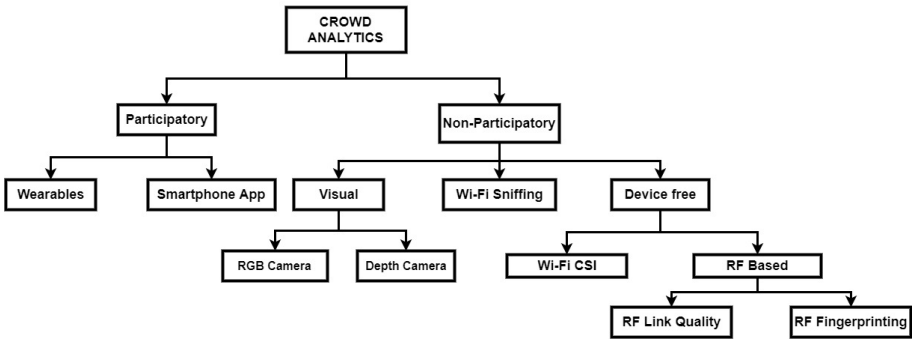

Figure 2.1: Tree diagram showing different approaches for crowd density estimation

Figure 2.1 shows a bird's eye view of various possible approaches to infer crowd density information. When using a participatory sensing approach its difficult to expect complete cooperation from everyone in the crowd either by installing applications or using wearables. Although participatory approaches can provide more accurate results we rule out adopting them as they are limited by the amount of participation from the people in the crowd. It might also be difficult to presume complete cooperation as the crowd size increases. We would like to incorporate crowd data analytics as part of smart lighting grids hence one of the main requirements is for the solution to be a part of light bulbs in the grid. This restricts the possibility of adopting device free approaches such as Radio Tomographic Imaging (RTI) with multiple sensors [40] or link based approach [15] as these require a Line of Sight between a TX-RX pair and the subjects to be tracked. This would not be possible if the sensors are mounted on the ceiling as part of a light bulb. WiFi CSI based approach requires modification to existing software stacks hence cannot be implemented on off the shelf hardware. Thus we select passive Wi-Fi sniffing as a suitable mode for gathering data as it can be easily implemented on most of the commercially available Wi-Fi hardware and does not require any active participation from the users. Due to growing adoption of smartphones among people we can expect most of the people to possess a smartphone with them all the time. The sniffers can be incorporated in the light bulbs and mounted on the ceiling.

Chapter 3

System Model

This chapter provides a detailed description of our system architecture. Section 3.1 describes the basic building blocks of the crowd distribution system. The basics of 802.11 packet sniffing is described in Section 3.2. Section 3.3 provides an analysis of the packet diversity and inter-packet interval for different smartphone configurations. Section 3.4 system challenges and their implications.

3.1 System Overview

Our approach to infer the crowd distribution in a given area is to count the number of smartphones with a Wi-Fi interface in the area of interest. As mentioned in Chapter 1, we assume that most people carry smartphones with them and have Wi-Fi switched ON. For this purpose, we deploy a network of Wi-Fi sniffers mounted on the ceiling as a part of the lighting grid. Each sniffer in the area passively listens to Wi-Fi packets in its vicinity. The sniffers are placed such that the Wi-Fi packets sent from a user's smartphone are captured by multiple Wi-Fi sniffers. All the sniffers in the area are time-synchronized with respect to a central node. The Wi-Fi packets are decoded to extract vital information such as MAC address of the device, time at which the signal was captured and the received signal strength (RSSI). These values from all the sniffers that received the signal are recorded in a database. The data thus collected is subjected to a number of post processing steps to infer people count in the target zone. Furthermore, the data is also used to estimate the position of a specific device.

Figure 3.1 provides an overview of the steps taken to perform crowd distribution analysis. Consider an area where four Wi-Fi sniffers A, B, C and D have been deployed at known locations. The Wi-Fi packets sent from the smartphone are captured by all the sniffers. In order to count the number of people, the data collected is subject to multiple filtering and post processing steps. To estimate the location of a user, the signal strength perceived by

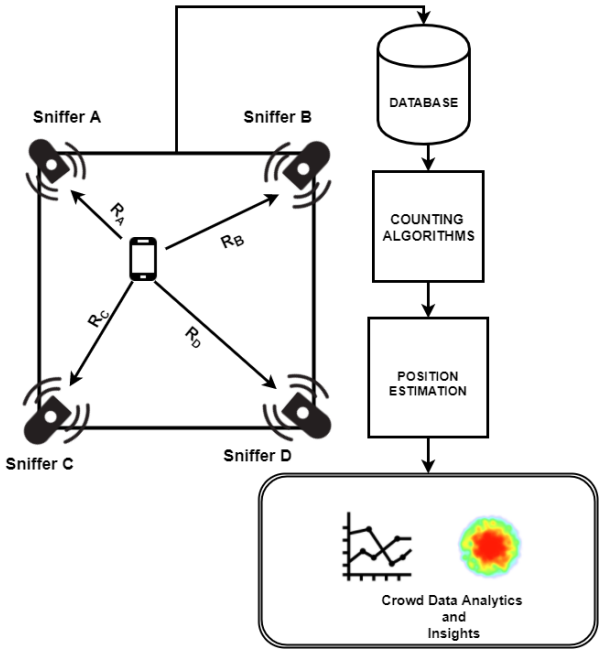

Figure 3.1: Architectural overview of the System

each sniffer is used for the localization algorithms. This enables us to understand both people count and spatial distribution of people. The information can be used to derive time based heatmaps and other crowd data analytics such as peak hours estimation, location of most crowded areas of the building.

3.2 802.11 Packet Sniffing

We make use of passive Wi-Fi scanners to capture the Wi-Fi packets. In order to achieve this, a wireless network interface is initialized in 'monitor' mode, in which all the on-going traffic in the wireless network can be captured while being non-intrusive and without associating itself to any network.

Figure 3.2 shows a simplified version of the IEEE 802.11 frame format [1]. The fields *Type* and *Subtype* denote the type of received frame.

The IEEE 802.11 standard mainly uses three types of frames for communication between an access point and an end-user device.

- **Data frame:** These frames carry data from the higher layers within their frame body.
- **Control frame:** These frames assist in the delivery of data frames between stations. These frames do not possess a frame body. The

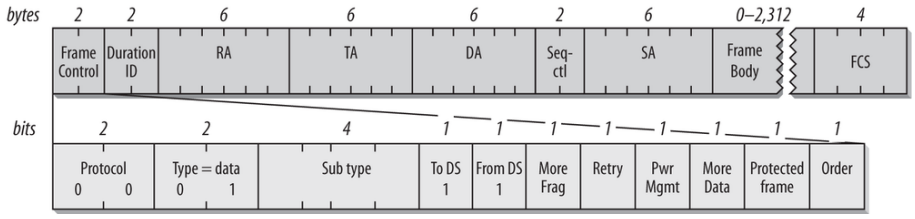

Figure 3.2: 802.11 frame format

frames are used to send acknowledgement (ACK, Block ACK), and coordinate access control among stations (RTS and CTS).

- **Management frame:** These frames enable stations to initiate and maintain communication among themselves. Actions such as authentication, de-authentication, re-association with access point are among the common types of 802.11 management frames.

There are several sub-types of each frame type with very specific functions [1]. We discuss few important frame types that are of interest in our problem context.

- **Probe request/response:** These are a type of 802.11 management frame that are used to detect access points and also used to connect to an access point. As a part of the active network scanning process, stations send a probe request frame on all the channels asking about the networks available on those channels. A probe request can contain the name of the network (SSID) a station it is trying to associate with, along with other metadata. Smartphones usually contain a list of previously remembered SSIDs which they try to probe along with other information such as its supported data rates. Probe requests are transmitted more aggressively when a smartphone is not associated with an access point. The frequency is reduced when its connected. A detailed analysis is given in later sections. An access point responds with a *Probe response* acknowledging the probe request packet and the data rate in which it wants to initiate communication.

- **Beacon frames:** Beacon frames are management frames that are periodically broadcast by the access points to advertise their presence. Beacon frames are sent only by the access points.

- **Null Data frames:** Null Data frames are a special type of frames in 802.11 WLANs. They are data frames which carry no specific data payload. Null Data frames are interesting for several reasons. They are only transmitted by end-user devices. They are used in a wide variety of applications such as power management, channel scanning, and to

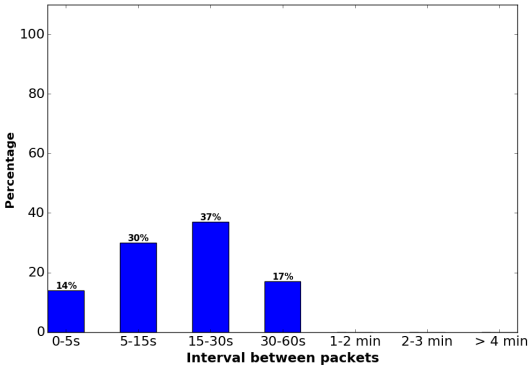

Figure 3.3: Inter-packet interval for probe request when disconnected from an access point

kepp the association alive. When used for keeping the association alive, mobile stations transmit Null Data frames to inform AP its presence during idle periods. This behaviour enables us to track smartphones even when they are associated with a network.

3.3 Smartphone Sniffing Behaviour

Each smartphone might behave differently depending on its configuration. This results in different Wi-Fi packet types and inter-packet intervals. We designed a series of experiments to understand the kind of packets sent by a smartphone under different configurations such as associated to a network, disconnected from a network, and without any Wi-Fi activity. The data was collected for at least 10 hours for each configuration. This information is required to understand the bounds of the system including the best case, the average case and the worst case scenarios.

3.3.1 Inter-packet interval and Packet Type

We wish understand the rate at which smartphones send packets under different configurations. The results from the three main types of configuration are discussed in this section.

Configuration : Disconnected from a Network

In this configuration, a smartphone's Wi-Fi is switched ON but not connected to any access point. When a smartphone is disconnected from the network, it frequently transmits probe requests on all the available channels for a specific frequency band (2.4Ghz/5Ghz). It can be a broadcast packet

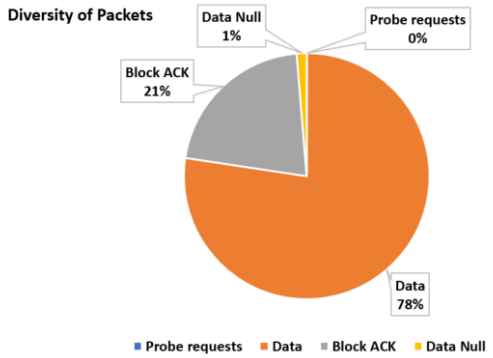

(a)

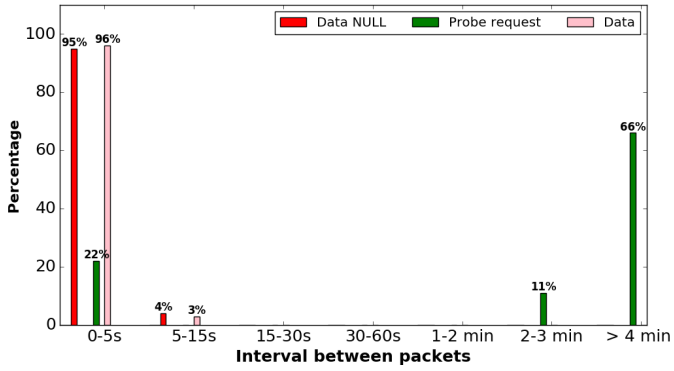

(b)

Figure 3.4: Diversity of packets and inter-packet interval when streaming applications are used

without any specific SSID or trying to connect to one of the previously remembered SSIDs. It was also observed that probe requests are triggered by the phone each time its unlocked by the user.

Figure 3.3 shows the interval between probe request packets from two different models of phone. It can be observed that any two intervals are vastly different. However, on an average we can expect a probe request every 30 - 60 seconds.

Configuration : Connected to a Network with Wi-Fi Activity

In this configuration, a smartphone is connected to an access point and applications are run such that there is a constant Wi-Fi traffic. This simulates situations where people might be listening to music on a streaming service or watching a video. In such conditions, smartphones generate a variety of Wi-Fi packets such as Block ACKs, Data, and ACK in very short intervals.

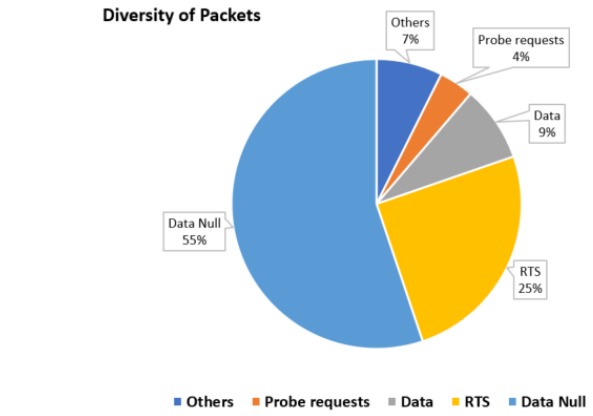

(a)

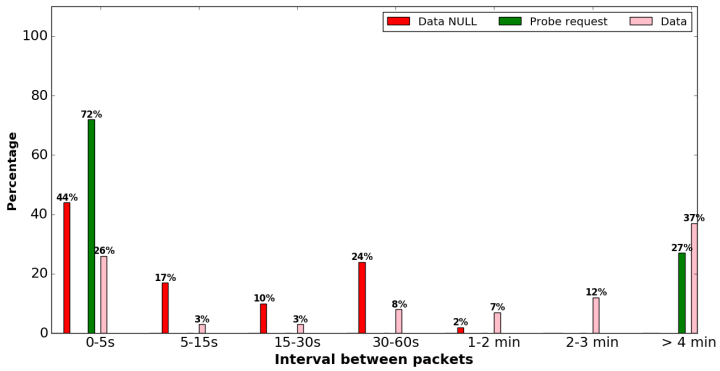

(b)

Figure 3.5: Diversity of Packets and inter-packet interval when Wi-Fi is ON but no user applications are running

It can be noticed that probe requests are still triggered even after associating with an access point.

Figure 3.4 shows the diversity of packets while streaming applications such as Youtube or Spotify are used. Data and Block ACKs dominate the sniffed packets. This can be regarded as the best case scenario as the packets arrive almost every second.

Configuration : Connected to Network and No Wi-Fi Activity

This is similar to the previous configuration, except no applications are run either in background or foreground. This can simulate a situation where someone is keeping their phone idle while being associated to a network. During such scenarios, Null Data and probe request packets are more dominantly seen with a few data packets every now and then perhaps due to the

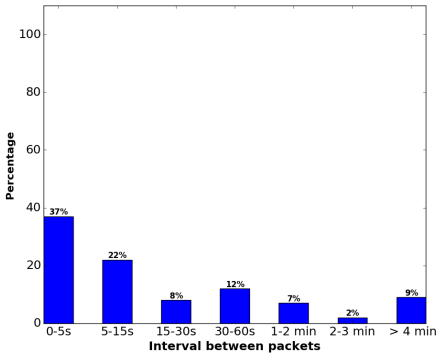

Figure 3.6: Interval between probe request packets from over 3000 devices

reception of messages/email etc. Null Data packets are sent by smartphones to inform their presence under idle conditions.

Figure 3.5 shows the different packet types and interval between those packets when the phone is idle without any activity or human intervention for close to 15 hours. The Null Data packets dominate in this configuration with the majority of packets arriving within 30-60 seconds. This enables us to sniff reliably devices even when they are connected to an access point.

A generic Scenario

In order to understand better, a generic scenario without limiting to any specific configuration was considered. Here, the interval between probe requests was analyzed from a probe request data set. The data set was collected from Crawdad repository [26]. The data from several real world scenarios such as a political meeting in Rome, St. Peter's Square in Vatican city, train station at Roma Termini central station etc were analyzed.

Figure 3.6 shows the interval between probe request packets that was obtained from the Crawdad dataset for close to 3000 devices. It can be seen that more than 50% devices have inter-packet interval within 30 seconds.

3.4 System Challenges

We want to use Wi-Fi sniffers as a part of the lighting grid in the target area. This imposes a set of challenges and constraints on the system. In this section, we go through these challenges and take design decisions because of the imposed constraints.

3.4.1 Un-cooperative nature of smartphones

We would like to understand the crowd distribution at a given location in a non-intrusive manner. Thus we do not posses any control over the smartphones. As a result, we have no control when a specific smartphone might send a packet or how many packets might be sent. A series of experiments were conducted to understand the types of packets and variation of the interval between packets for several phones in order to understand the best, average and the worst case scenarios. The results from the section 3.3 indicate that a minimum sampling interval between $30 - 60$ seconds is desirable for the system as most of the phones would have transmitted by this interval. A lower resolution bears the risk of losing data.

3.4.2 Limited information

Due to the non-intrusive nature of sniffing, many characteristics of a transmitting smartphone such as transmission power, antenna directionality, antenna height and orientation are unknown for any given smartphone. We summarize some of these characteristics.

- **Antenna characteristics :** A majority of smartphone vendors place the Wi-Fi antenna at one of the corners of the phone body. This results in an uneven RSSI distribution around the device leading to the RSSI values being significantly higher in certain directions as compared to the others.

  An experiment was conducted to verify the extent of such variations by placing a smartphone at different orientations with respect to the sniffer and collecting RSSI values. Figure 3.7 shows the distribution of RSSI values at different orientations. It can be seen that difference is quite high in certain orientations as compared to the others. Such random variations can significantly impact the location estimation algorithms.

- **Transmission power:** The permissible limit for the maximum transmission power of a Wi-Fi device is governed by the FCC regulations [21]. The maximum permissible limit depends on several factors including antenna gain, and the frequency band used among other things. The maximum transmission (TX) power with an antenna gain of 6dBi is capped at 30dBm (1000mW) as shown in Table 3.1. However, since the TX power has a direct impact on the battery consumption, the smartphone vendors do not keep the TX power at maximum all times. For instance, the TX power will be considerably reduced in 'low battery' mode as compared to a 'performance' mode. These variations in the TX power may not be uniform across all the vendors. Thus, range based estimation methods will be prone to errors due to

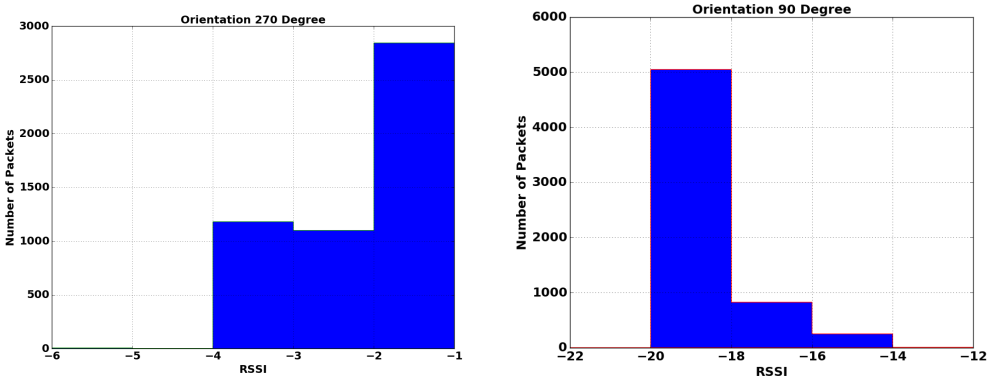

(a) (b)

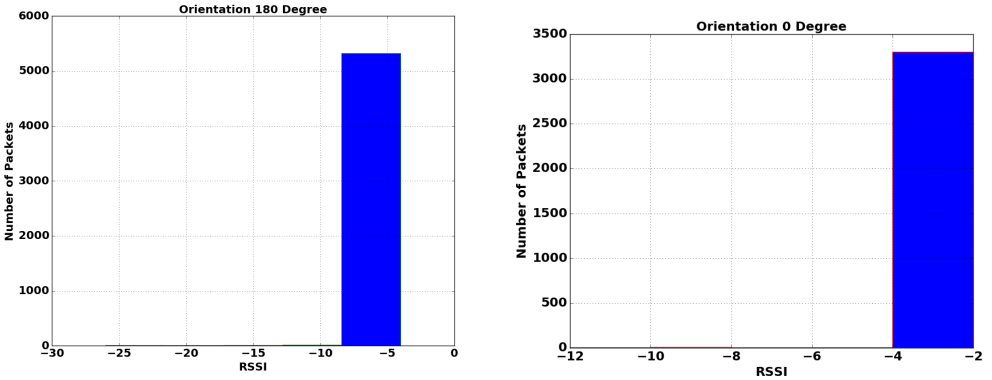

(c) (d)

Figure 3.7: Variation in RSSI values at different orientations between sniffer and smartphone.

variations in the TX power. Radio fingerprinting based estimation methods may also suffer as fingerprint database built with one device cannot be used for other devices.

Transmit Power (dBm)	Antenna Gain (dBi)	EIRP (dBm)
30	6	36
29	9	38
28	12	40
27	15	42
26	18	44
25	21	46
24	24	48
23	27	50
22	30	52

Table 3.1: FCC guidelines for TX power for 2.4GHz band

- **Passive sniffers:** The sniffers are meant to be passive which means they only listen to the Wi-Fi packets in the area. The sniffers will not engage in any communication with the smartphones to increase the packet generation rate. Due to this, we might miss close to 10-12% of the devices while counting the number of devices if as they send data at lower intervals as seen in Section 3.3. Since there is no direct communication between sniffers and the smartphones hop based localization algorithms cannot be considered.

3.4.3 COTS sniffing hardware

We intend to build a system that uses commercially available off-the-shelf hardware. Our system does not use any sophisticated directional antennas and is designed to work with any standard Wi-Fi chipset available in the market. As a result, we can only rely on the collected (timestamped) RSSI values which is commonly exposed by every off the shelf Wi-Fi chipset. This limits us to use only RSSI based localization algorithms.

Chapter 4

People Counting

This chapter describes our proposed methods to infer the people count using Wi-Fi sniffing. Section 4.1 describes the architecture and the approach used. Section 4.2 describes various challenges faced when Wi-Fi sniffing is used for crowd density estimation. Section 4.3 describes various filtering mechanisms to arrive at an approximate people count. Section 4.4.2 describes the results obtained from the testbed and the live experiments. Finally Section 4.6 describes some of the limitations of the approach used for people counting.

4.1 Introduction

Our approach for counting people is to count the number of smartphones with a Wi-Fi interface in the area of interest. For this purpose, we deploy a network of Wi-Fi sniffers in the area that passively listens for Wi-Fi packets in its vicinity and uploads the data to a central node. The data thus collected is subjected to a number of filtering and post-processing steps to infer the people count in the target zone. Figure 4.1 represents the building blocks for people counting by means of Wi-Fi sniffing.

4.2 Challenges

The following section describes various challenges encountered when we try to deduce people count by sniffing Wi-Fi packets in the vicinity.

4.2.1 Increasing number of Wi-Fi devices

The number of devices with a Wi-Fi interface has increased significantly over the years and this number is predicted to increase further. When we try to sniff for Wi-Fi packets in such a scenario, we see a large number of devices that get discovered in our vicinity. Generally the number of Wi-Fi devices is much more than the number of people in a given area. This is due

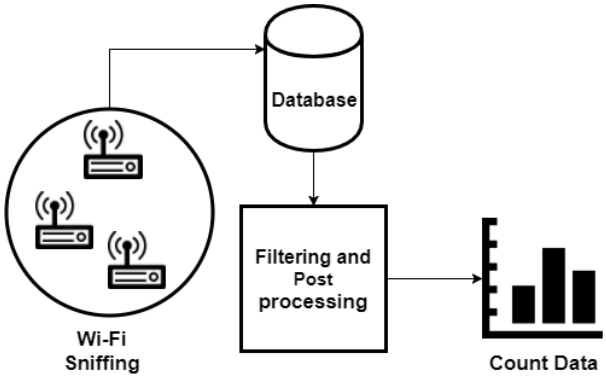

Figure 4.1: Building blocks of people counting system using Wi-Fi Sniffers

to the presence of many devices other than smartphones including laptops, tablet computers, routers, Wi-Fi repeaters, and other smart devices with Wi-Fi capabilities.

We performed a sniffing experiment in an event where there were approximately 68 people present. Figure 4.2 depicts the number of unique Wi-Fi devices detected every 5 minutes. As can be seen in the figure, the number of detected devices is much more than the average number of people in the area.

4.2.2 Devices outside Target zone

Since Wi-Fi sniffers have a large range (around 100m), the sniffers will be able to detect even devices which are outside the target zone. These may include people who are just passing by around the target area.

Consider a situation shown in Figure 4.3. It is important to ignore the passer by devices as it may impact the count severely depending on how many devices are outside the area of interest.

4.3 Filtering mechanisms and Post Processing

This section describes the different filtering mechanisms and post processing steps we propose to use in order to avoid counting unwanted devices in and around the area of interest.

4.3.1 Filtering based on Wi-Fi Packet type

Consider the pie chart shown in Figure 4.4 depicting the different types of Wi-Fi packets encountered during a typical sniffing session that collected close to 2 million packets.

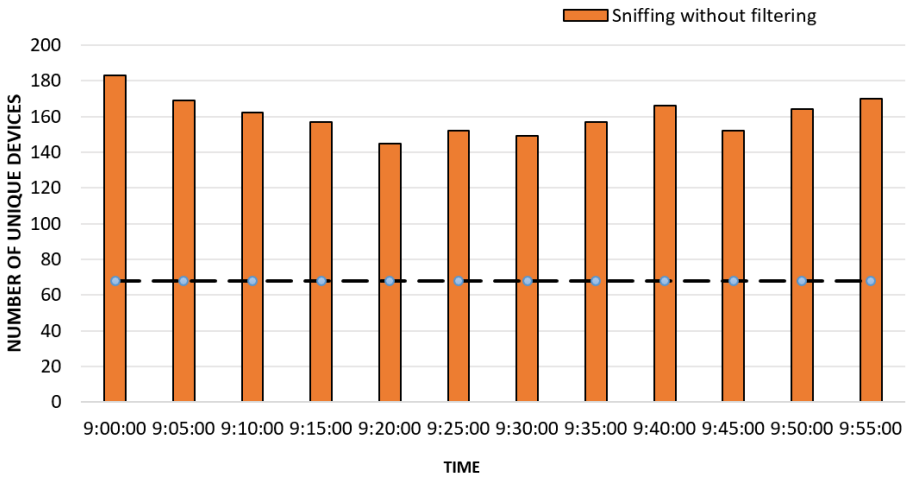

Figure 4.2: Number of unique devices detected in an event of approximately 68 people

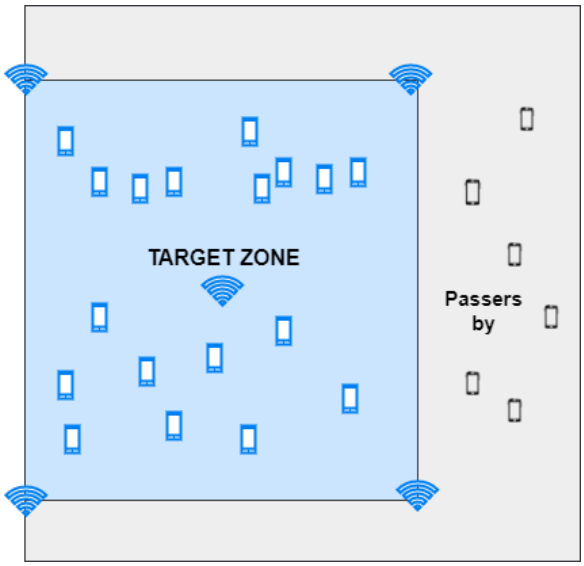

Figure 4.3: Stray devices outside the area of interest

As it can be seen from Figure 4.4, a majority of the packets are data packets constituting around **32%** followed by Beacon frames and Probe Response packets which constitute roughly **18%** and **12%** respectively. The Beacon frames and Probe Response packets are typically transmitted by Wi-Fi routers hence can be ignored. Removing these would reduce the size of data set by **31%**.

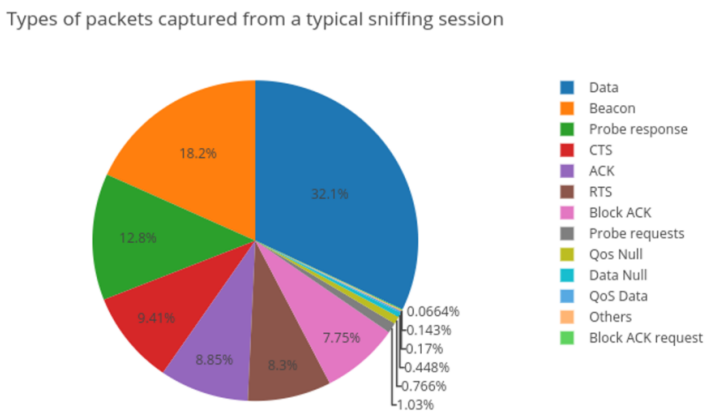

Figure 4.4: Types of Wi-Fi packets encountered during sniffing

.

4.3.2 Filtering based on Proximity and Manufacturer Identities

To avoid detection of the devices that are far away from the target zone, we propose to set an RSSI threshold for each sniffer. The threshold is chosen such that we avoid detection of very weak signals which probably might originate either from a far away device or a device which might be on the other side of a thick wall. The attenuation of signals from a wall can be between 10-15dB [32].

The area of interest is surveyed and measurements are taken both inside and outside the target zone in order to select an optimal threshold. This can be done during the lighting grid installation phase. It can be tweaked based on the area and required sensitivity. In our experiments, the test setup was in a room 10m in width and 14m in length. In order to avoid detection detection of far away devices we can put up a threshold of -75dB. All signals that are below this threshold are ignored.

The first three octets of a detected MAC address represents a unique identifier called as Organizationally Unique Identifier (OUI) number. It is a 24-bit number that uniquely identifies the manufacturer, or other organization responsible for the Wi-Fi chip. IEEE maintains a database mapping OUI numbers to their manufacturer identities [24]. For instance 3CD92B belongs to HP, 0050BA belongs to D-Link corporation and so on.

Many static devices within the target zone such as routers, smart television, printers can be blacklisted based on such manufacturer identities. To further reduce the dataset and remove static devices we use time based blacklisting approach. Each day a blacklist file is built up containing newly detected OUIs. A time is chosen such that no activity from people is seen,

for instance every night between 2AM to 4AM would be a probable time where Wi-Fi activity will be mostly because of static devices in the area and not from people in the vicinity. All these devices are put in a blacklist so that they can be ignored when they are detected next time.

Figure 4.5 shows the most frequently seen OUI everyday between 00:00 AM - 04:00 AM. It can be seen that a set of OUIs keep appearing regularly every night such as 003A7D, 004268 etc. These consequently belong to Cisco Systems which is a popular vendor of wireless routers. Thus we can remove a large percentage of static devices in the vicinity by using time based blacklisting approach.

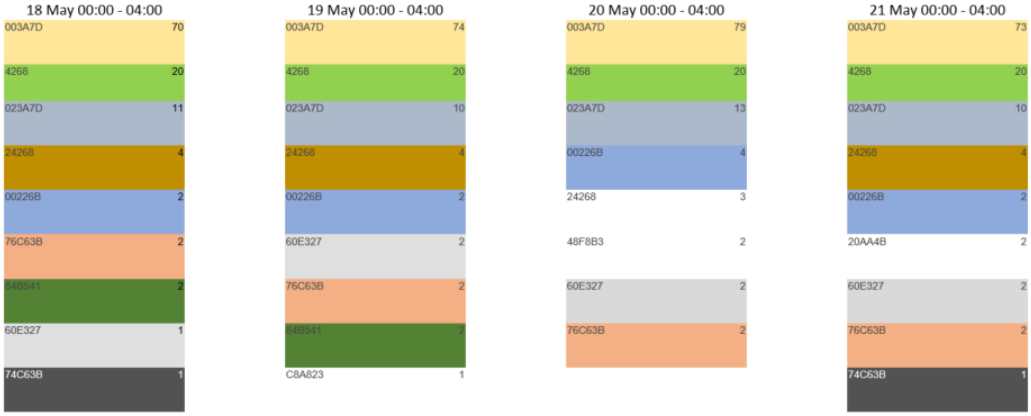

Figure 4.5: Frequently seen OUIs every night between May 18 and May 21

Combining all the above filtering mechanisms we can reduce the data set by more than **60%** as seen in Figure 4.6.

4.3.3 Avoiding Stray Devices

After various levels of filtering as discussed in the previous sections, there might still be false positives due to passers by and devices just outside the target area as discussed in Section 4.2.2. In order to reduce the number of false positives we try to estimate the dwell time of each device. Devices which just passed by will be detected for a very short interval resulting in lower values of dwell time.

To further reduce the number of false positives, we only take into account devices which were detected by multiple sniffers after applying an RSSI threshold. Consider the configuration shown in Figure 4.7 the detection range of each sniffer after application of an RSSI threshold is represented by circles around the sniffer. When a device is within the target zone, it is

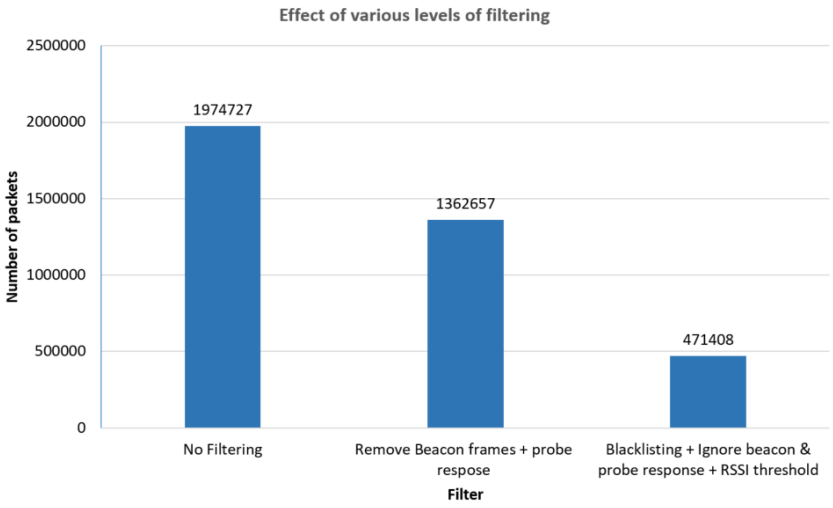

Figure 4.6: Reduction in Dataset size after each stage of filtering

detected by multiple sniffers. When a device is very far away it is unlikely that it will be detected by any sniffer after an RSSI threshold. Similarly if the device is detected by only one or two sniffers, it can be assumed that it is outside our target zone. In Figure 4.7 smart phone **A** will be seen by three sniffers where as smart phone **B** will be seen by only one sniffer. Thus we can categorize smart phone **A** to be within the target area and ignore smart phone **B** to be outside and thus not take it into account while counting.

The algorithm for counting is presented in Algorithm 1. Let **start_time** and **end_time** denote the time intervals within which we want to count the number of smartphones with a sampling interval given by **sample_interval**. **Database** contains Wi-Fi data sniffed from smartphones.

4.4 Experiment Setup

In order to verify the counting algorithms, data was gathered both in controlled and real environments. A set of experiments were conducted at the Wi-Fi testbed at the University of Ghent. Another set of experiments were conducted at a live testbed that was set up at a coffee corner and an auditorium at Philips Lighting research building in Eindhoven.

4.4.1 W-ilab Testbed Configuration

The w-iLab.t (short name: wilab) is an experimental, generic, heterogeneous wireless testbed deployed in the iMinds building in Ghent, Belgium [8]. It provides a permanent testbed for development and testing of wireless applications via an intuitive web-based interface. There are 44 testbed nodes

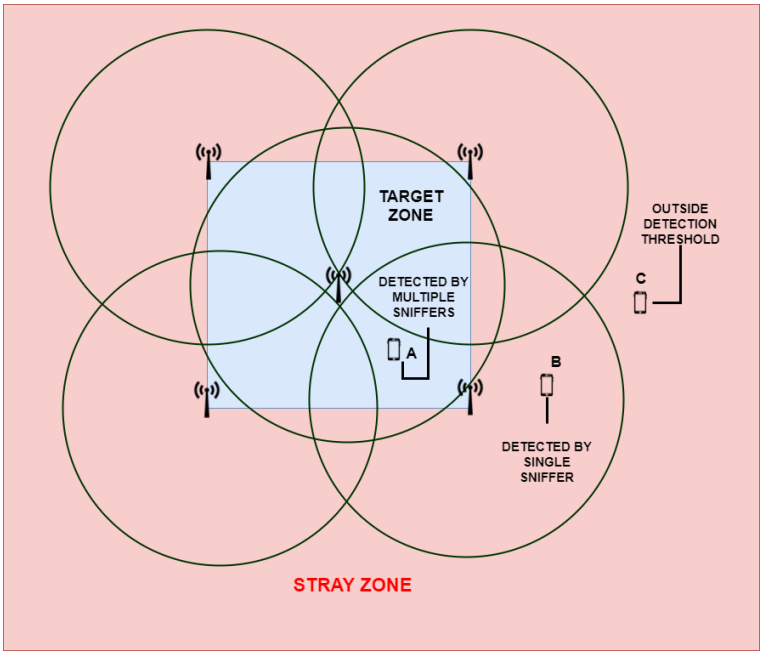

Figure 4.7: Avoiding detection of devices outside target area

which are mounted to the ceiling of the data center of the iGent building (in Ghent): a 30m by 10m room in a grid configuration with horizontal separation of 2.5m and vertical separation of 2meter.

The nodes are generic wireless nodes which can be configured to behave as either as a Wi-Fi device or as a sniffer. For our experiments, we indicate a zone of interest and place a number of sniffers within the zone. A set of nodes are programmed to send Wi-Fi packets which are captured by the sniffers. All the data is gathered at a central node to be used later for analysis.

The test configuration shown in Figure 4.8 has five nodes that act as Wi-Fi sniffers, an access point and a set of 28 nodes that are configured as devices. Among these nodes 17 are present within the target area and 11 nodes outside the zone of interest which we call as the stray zone. The Wi-Fi devices are programmed to send Wi-fi packets at different intervals such every 1 s, 30 s, 60 s etc. The detailed configuration of the nodes can be seen in Table 4.1.

4.4.2 Testbed Results

The data collected using the configuration shown in Figure 4.8 is subjected to several post processing steps as mentioned in the previous sections. The resulting graph containing count is shown in Figure 4.9. The number of devices within the target area is 17. The time window is chosen to be 5

Algorithm 1: Get Device count between a given duration

```
Require: start_time,end_time, Database
  while t ==sample_interval do
    device_count = 0
    Extract data between start_time and end_time from database
    unique_devices =  get_unique_devices(start_time,end_time)
    for device in unique_devices do
      dwell_time= (time_last_detection - time_first_detection)
      sniffer_count =
      get_detected_sniffer_count(interval_start,interval_end)
      if  dwell_time ≥ dwell_time_threshold and num_sniffers ≥
      sniffer_threshold then
        device_count = device_count + 1
      end if
    end for
  end while
```

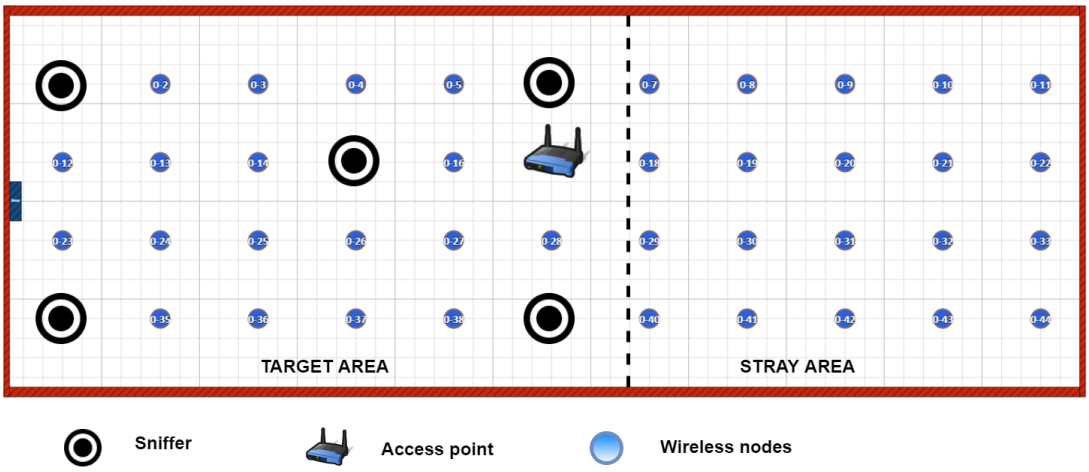

Figure 4.8: Configuration of nodes at W-ilab testbed

minutes as all the devices would have transmitted a packet at least once during this time interval resulting in a stable count. The data was collected for a duration of 1 hour, dividing this into five minute intervals a device should be detected at least 12 times.

The secondary axis shown to the right depicts the number of unique devices seen in five minute intervals without any post processing. This number is quite large as it contains all types of devices including routers, printers and many random smart devices with Wi-Fi. Each node in the testbed has multiple Wi-Fi interfaces and also virtual interfaces hence the large number. The primary axis to the left shows filtered count obtained

Testbed Configuration	
Number of Sniffers	5
Number of devices with target zone	17
Number of devices outside target zone	11
Channel Frequency	2.412GHz
Device configuration - Target zone	
Interval	Number of Devices
10	4
30	4
60	5
300	4
Total	17
Device Configuration - Stray zone	
Interval	Number of Devices
30	11

Table 4.1: Device configuration and packet interval for devices at w-ilab testbed

after post processing along with the ground truth. This can be attributed to RSSI fluctuations due to which devices get ignored during certain intervals as shown in Figure 4.10.

Selecting a threshold for RSSI and the number of detected sniffers is a crucial step. Figure 4.10 shows the effect of RSSI threshold and the number of detected sniffers on counting algorithms. The ground truth here is 17 devices, the blue bars indicate the value given by counting algorithms and red bars indicate the number of false positives detected. Selecting a lower threshold for detected sniffer count increases the number of false positives within the zone of interest. For instance, when the RSSI threshold is $\leq$-50dB and seen by at least 3 sniffers, we are able to detect all 17 devices within the target zone but we also bring 11 stray devices into the system. Therefore a sweet spot has to be found which can give us as less stray devices as possible with an acceptable accuracy. In the graph we can see that having a sniffer count of 4 with an RSSI threshold of $\leq$-50dB can give optimal count value while keeping the false positive count low.

4.5 Results from the Live Experiment

In order to evaluate the algorithm in real word scenarios, we deployed Wi-Fi sniffers at an event involving people at an auditorium and a coffee corner in an office building.

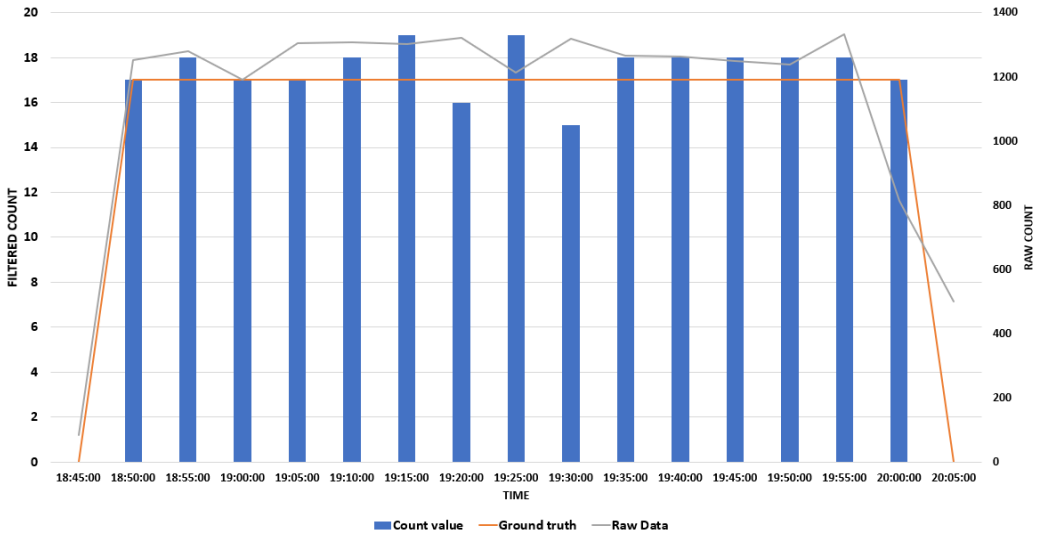

Figure 4.9: Graph showing count results before and after filtering. The secondary axis shows the raw count and primary axis show the filtered count against time

4.5.1 The DoVo Room

The DoVo is the weekly Philips internal seminar series from Philips Research, and takes place every Thursday. The name DoVo is an abbreviation for the Dutch word **Donderdagochtend-Voordracht** (Thursday Morning Lecture). This gathering takes place in an auditorium which is 10m x 14m with a capacity of approximately 120 people. We deployed 3 sniffers in the room and gathered Wi-Fi sniffing data during the event. The people count obtained after post processing is shown in Figure 4.12. The ground truth was collected by manual counting during the event.

In Figure 4.12, it can be seen that the algorithm closely follows the ground truth estimation. However during peak times, it can seen seen that the estimated people count is much less than the actual count. Upon surveying people, two reasons were found. A number of people who attended the event never brought their smartphones with them (especially most of the ladies reported that they left their phones on the desk). An announcement was made about the ongoing experiment and Wi-Fi sniffing to have a consent from people. Several people switched their Wi-Fi off as they were paranoid about privacy reasons.

4.5.2 Coffee Corner

Wi-Fi sniffers were deployed in the coffee corner area shown in Figure 4.13 where people generally gather throughout the day. The area is relatively small with dimensions 6.5m x 9m, five sniffers were deployed in this location.

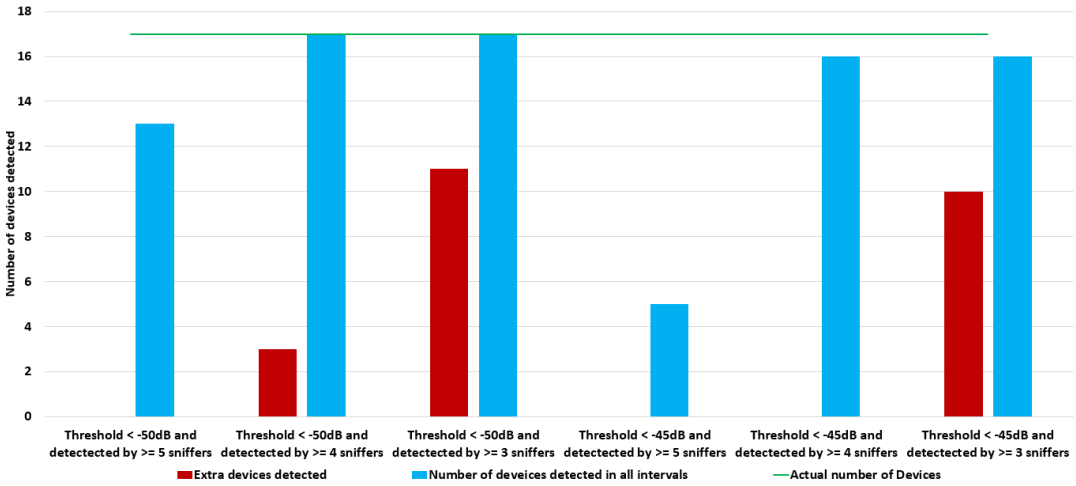

Figure 4.10: Effect of RSSI threshold and sniffer count on counting algorithms

The ground truth was collected using Xovis people counting cameras, these are depth sensing cameras used for people counting.

The Wi-Fi data was collected for 6 hours from 8:00 AM till 14:00 PM. The graph obtained after applying the counting algorithms is shown in Figure 4.14. The count values are superimposed against values obtained from the camera. From the graphs, it can be seen that the output from the counting algorithms match the trends seen by the camera throughout the day. The values seen from the camera and the counting algorithms might differ because of the following reasons.

- **Dwell Time :** The counting algorithms take into account the dwell time estimates of a device as explained in Section 4.3.3. The devices are ignored if the dwell time is less than the established threshold. Here the threshold was chosen to be 60 seconds. Any device with dwell time less than 60 seconds would not be counted. However camera would still count irrespective of the dwell time of a person. If somebody grabs a coffee quickly and goes away from the coffee corner this would be counted by the camera but may not be recorded by the sniffers.

- **Camera coverage area :** The coverage area of the cameras is much lesser than the Wi-Fi sniffers. The cameras typically cover only 25% of the entire coffee corner area. Thus people present in such areas might be counted by sniffers and not by cameras.

(a) (b)

Figure 4.11: The DoVo room where weekly lectures takes place

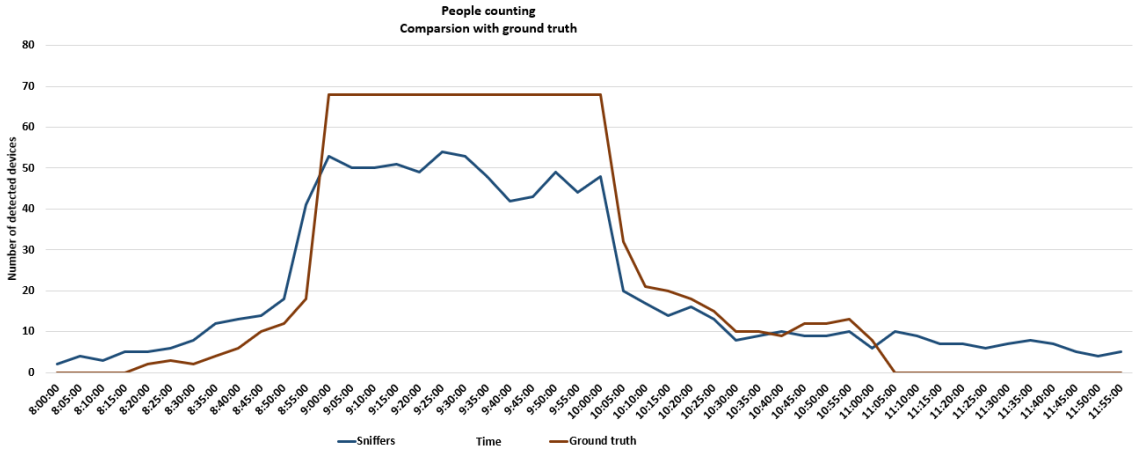

Figure 4.12: Graph showing count results at a DoVo event with the manual ground truth

Figure 4.13: Wi-Fi sniffers and cameras deployed in the coffee corner area

4.6 Limitations and Corner cases

Various experiments were conducted both in controlled environment such as W-ilab testbed and real world situations such as DoVo room and the coffee corner. From the results, it can be inferred that the counting algorithms provide a fair estimate of number of people in a given area. However, these algorithms have several limitations and certain corner cases which need to be considered.

- The counting algorithms work on an underlying assumption that most of the people carry their smart phones with them and have their Wi-Fi switched on most of the time. From our live experiments, it was found this may not be true in many cases. In coffee corner case it was observed that several people who came to grab a coffee never had their smart phones with them. This ratio might differ depending on the type of event and the location as well. The count values may be radically inaccurate in an event comprising of mainly children or elderly who generally don't have smartphones. However the counting algorithms may perform much better an event such as a music concert or a football game in an arena where majority of the people have their smartphone with them and there is lot of activity on the Wi-Fi activity in the area.

- Time based blacklisting is used to remove a lot of static devices. It has been noticed that several new static devices that are not smartphones keep appearing regularly. Therefore it is important to constantly update the blacklist file with new devices frequently. A stale blacklist file may impact the accuracy of counting.

- Selecting a threshold for RSSI and dwell time estimates can be very

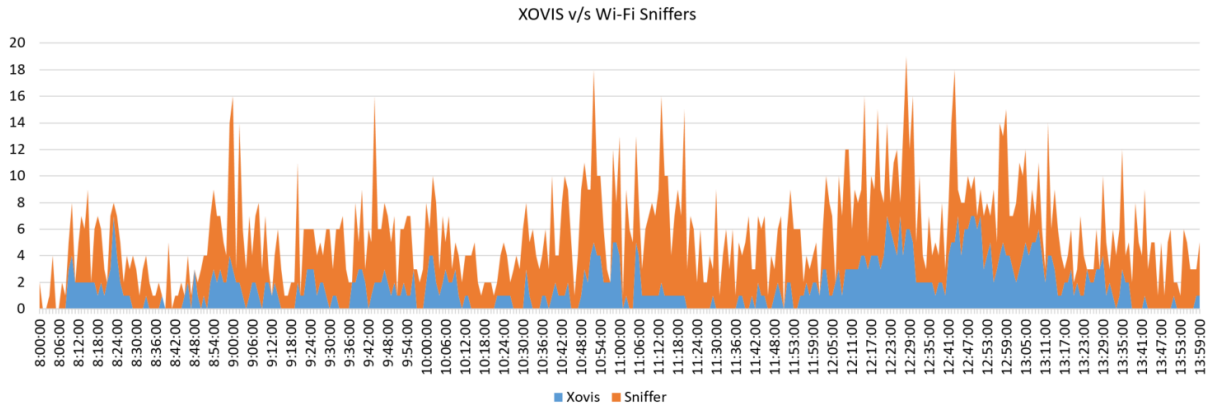

Figure 4.14: Count data obtained from Wi-Fi sniffers and ground truth from Camera

tricky. Since RSSI is subject to fluctuations as explained in Section 4.4.2, several devices may not be detected in certain intervals of time due to low RSSI values. At the same time relaxing RSSI threshold will increase the number of false positives as more area is covered by the sniffers. Similarly selecting a threshold for dwell time can also lead to inaccuracies in counting. Due to diverse nature of smart phones the packet interval might differ for each smart phone as established in previous experiments. If the dwell time threshold is chosen to be too low then certain devices may be ignored because of their low packet transmission rate although they are inside the target area.

- Several vendors follow procedures such as MAC address randomization to avoid tracking of smart phones. These might introduce some level of inaccuracy to the counting algorithms. However it has been found that such procedures is employed bu only certain vendors in only few models.

Chapter 5

Inferring Crowd Distribution

This chapter describes algorithms to infer the spatial distribution of people in a given area. Section 5.2 provides an overview of the challenges in position estimation. In Section 5.4, the localization algorithms used and the obtained results are described. A comparison of the localization algorithms are provided in Section 5.5. Section 5.6 describes methods to generate confidence scores to assess the reliability of position estimation.

5.1 Introduction

Crowd distribution refers to the approximate locations where people might be present in a given area. The counting algorithms discussed in Chapter 4 give us information only about the number of people in a given space. However, knowing the spatial distribution along with the people count can give us sufficient data to make many crucial decisions. For instance, counting algorithms combined with spatial data can help us in understanding where the most busy areas of a given space are. It can help us allocate the resources intelligently based on the crowd distribution. We can perceive how the crowd distribution might change over a period of time. This information is derived based on localization of smartphones that users carry with them.

5.2 Localization Challenges

Localization has been a highly active area of research since many decades and there exists a plethora of approaches to localize a device/person. However, the constraints imposed on the system has direct implications on the selection/design of the localization algorithms and their accuracy. In this section, we briefly summarize the effect of these constraints and their relation with localization.

5.2.1 RSSI Approach

Since we choose Wi-Fi sniffing as our preferred approach to gather data, the only information that is available about an unknown node is the timestamped RSSI values from multiple sniffers. Fine grained information about the node such as Time Difference Of Arrival (TDOA), Angle Of Arrival (AOA) are unknown. Thus, we cannot use TDOA/AOA based localization algorithms like Katabi et al. [37], Rong et al. [31]. Due to these constraints, we are restricted to use only RSSI based localization approaches. RSSI is known to be prone to large and small scale variations due to multipath and reflection of signals. It may also vary depending on the orientation and position of the smartphone. This may lead to inaccuracies in location estimation.

5.2.2 Time resolution and Frequency of Packets

As our approach is non-intrusive in nature, we do not possess any control over how many packets might be sent from a smartphone at any given time. From our previous experiments in Section 3.3 of Chapter 3, we conclude that the majority of the smartphones send a packet every 30 - 60 seconds. However, there will always be a certain percentage of smartphones that send packets at a reduced rate.

The number of packets received heavily depends on the configuration a smartphone is in: a large number of packets can be expected during data transfer where as fewer packets during idle or low battery mode. Having more number of packets gives us the ability to mitigate the effects of RSSI variation by applying appropriate filtering and smoothing mechanisms. However, a large number of packets cannot be assumed to generated from each smartphone all the time. Due to these factors, the accuracy of localization might be non-uniform among the discovered smartphones.

5.3 Experimental Setup

In order to efficiently analyze localization algorithms, a relatively large space is required in which we have sufficient freedom to measure dependency of algorithms with respect to various factors such as topology of sniffer placement, number of sniffers in the area etc. In order to achieve this we decided to make use of a Wi-Fi testbed where we can perform effective emulation. We found Wilab2 testbed [8] to be the most appropriate for this purpose. It is a generic, heterogeneous wireless testbed similar to the one used in 4. It can be found in an unmanned utility room (size: 61m x 22m) and consists of over 120 fixed Wi-Fi nodes mounted close to the ceiling and 16 mobile robots that can be remotely controlled.

Figure 5.2 provides an overview of maximum number of sniffers that can be deployed in the area. In full scale deployment, the minimum separation

Figure 5.1: Wilab2 Testbed and Robots with Wi-Fi interface on them

between the horizontal sniffers is 6m and vertical sniffers is 3.5m.

This setup closely mimics spaces such as an arena concourse or an auditorium. Since the robots also have Wi-Fi nodes mounted on them they can be used to mimic the people moving or emulate crowd buildup at different locations. The data collected form the experiments are analyzed using different localization algorithms.

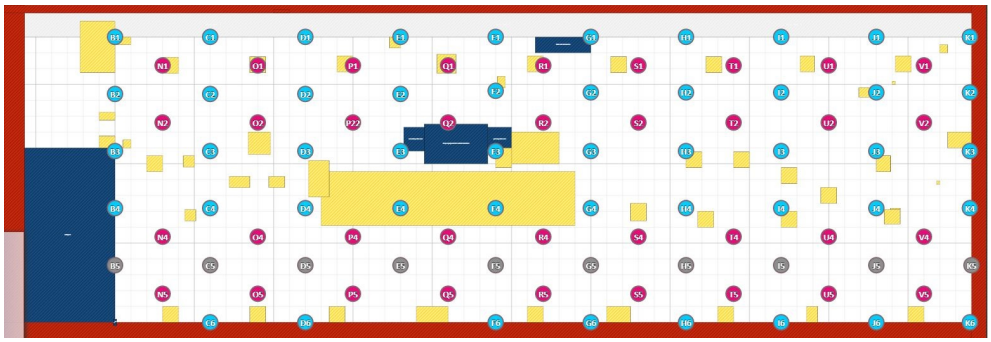

Figure 5.2: Overview of deployment of Wi-Fi sniffers at the testbed

5.4 Localization Algorithms

In this section, we describe the localization algorithms which were used to deduce the location of an unknown node. We propose enhancements to improve localization accuracy and its dependency on various factors.

5.4.1 Centroid Based Localization

Weighted Centroid Localization (WCL) has been used to determine the location of unknown nodes in many Wireless Sensor Networks (WSN) [6]. The algorithm has low execution time and computational complexity. WCL was proposed as an improvement over Centroid localization [10]. It determines the position of an unknown node by averaging the locations of known reference points also known as anchor nodes. In WCL, the weights are adjusted such that the anchor nodes closest to an unknown node gets more weight compared to the nodes that are farther away from the unknown node. This increases the location estimation accuracy.

Let $L_i(x_i, y_i)$ denote the location of i^{th} sniffer. Let d_i denote the distance between the unknown node and the sniffer S_i and g denote the degree which determine the contribution of each sniffer. The distance is raised to a power g so that weight of farther distances are marginally lower. Simulation run in [6] indicate an ideal value to be g =1. The weight w_i given to each sniffer S_i depends on its distance from the unknown node and the degree of contribution :

$$w_i = d_i^{-g} \tag{5.1}$$

The location $P(x, y)$ of the unknown node can be estimated using combined weights of all N sniffers as:

$$P(x, y) = \frac{\sum_{i=1}^{n}(w_i \cdot S_i)}{\sum_{i=1}^{n} w_i} \tag{5.2}$$

From Equation 5.1, it can be seen that WCL requires distance d_i to be calculated. This generally involves use of path loss models which can be prone to errors. If weights can be allocated solely based on RSSI values seen at each sniffer then we don't have to calculate actual distances based on path loss models.

The detected signal strength P_{RX} at a distance d can be calculated as :

$$P_{RX} = P_{TX} \cdot G_{TX} \cdot G_{RX} \cdot \left(\frac{\lambda}{4\pi d}\right)^2, \tag{5.3}$$

where P_{TX} is the transmitted power. λ is the wavelength of the radio signal. G_{TX} and G_{RX} refers to the antenna gains of transmitter and receiver respectively. Thus distance d can be estimated as :

$$d = \frac{\lambda}{4\pi}\sqrt{\frac{P_{TX} \cdot G_{TX} \cdot G_{RX}}{P_{RX}}} \tag{5.4}$$

The RSSI value can be expressed as a ratio received signal strength P_{RX} and reference power P_{ref} as:

$$RSSI = 10 \cdot \log \frac{P_{RX}}{P_{ref}} \tag{5.5}$$

$$P_{RX} = P_{ref} \cdot 10^{\frac{RSSI}{10}}. \tag{5.6}$$

Substituting Equation 5.6 in Equation 5.4, the new weight can be calculated as :

$$w_i = \frac{1}{d_i^g} = \frac{1}{\left(\frac{\lambda}{4\pi}\sqrt{\frac{P_{TX} \cdot G_{TX} \cdot G_{RX}}{P_{ref} \cdot 10^{\frac{RSSI_i}{10}}}}\right)^g} \tag{5.7}$$

After normalization, the new weight W_i is:

$$W_i = \frac{w_i}{\sum_{j=1}^{n} w_j} = \frac{\sqrt{\left(10^{\frac{RSSI_i}{10}}\right)^g}}{\sum_{j=1}^{n}\sqrt{\left(10^{\frac{RSSI_j}{10}}\right)^g}} \tag{5.8}$$

To further improve the estimation accuracy, the anchors whose RSSI values are lower are given even higher weights by modifying the above equation. Improved weights W_i' can be expressed as:

$$W_i' = W_i \cdot N^{2W_i} \tag{5.9}$$

Here $W_i \cdot N^{2W_i}$ is chosen to be the enhanced weight as $W_i \cdot N^{2W_i} > W_i$. Final estimated position with improved weights can be expressed as :

$$P(x, y) = \sum_{i=1}^{n} (W_i' \cdot S_i) \tag{5.10}$$

Figure 5.3 shows the scatter plot and CDF of localization error obtained when a sniffer was placed every 6 m with total of 52 sniffers in the area. The sampling interval was chosen to be 30 s. From the CDF, it can be seen that more than 60% of the time estimation error is below 3m.

Traditionally WCL algorithms are typically used in large scale WSN deployments; it takes into account only the anchor points in range of an unknown node to estimate the position. In our scenario, all the deployed sniffers are located close enough combined with long range of Wi-Fi. Therefore, a majority of them are always within the range at any given time. Errors will be introduced in position estimation if we take into account all the sniffers in the area. Hence, we take S sniffers out of the total N that receive the strongest RSSI. This number has to be chosen carefully.

Figure 5.4 shows the error in position estimation for different values of chosen S. The total number sniffers used in the experiment was 52. As S approaches the total number of sniffers in the area the estimation accuracy reduces. An ideal number would be 3 or 4 depending on the deployment topology. The topology used in our experiments is grid based deployment. Hence we can expect $S = 4$ to be an acceptable value. Thus the location is calculated according to Equation 5.10 only after sorting the RSSI values from the sniffers and taking values only from the N strongest sniffers.

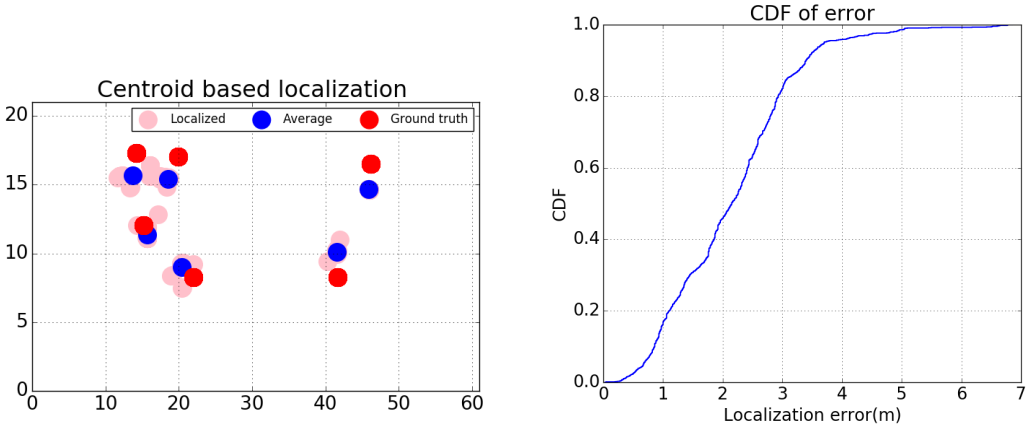

(a) (b)

Figure 5.3: Scatter plot of Localization and CDF of error

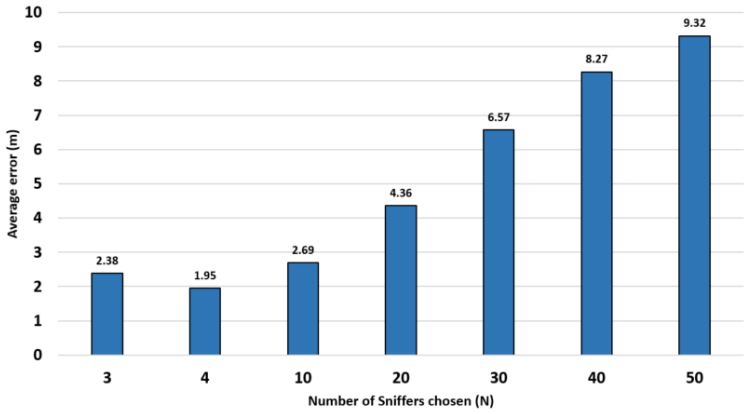

Figure 5.4: Variation of average error for a node as the value N approaches total number of sniffers.

5.4.2 Constraint Matching

Ecolocation algorithm proposed by Kiran et al. [48] is a range free localization algorithm. The algorithm was chosen due to it low complexity and a reasonable accuracy. The localization area is partitioned based on distance constraints. These constraints form a unique signature for different regions in the localization area. The location which has maximum number of satisfied constraints is then determined to be the best estimate of the unknown node's location.

Consider the situation in Figure 5.5 where A,B,C,D and E represent anchor nodes whose location is known and L represents the location the node

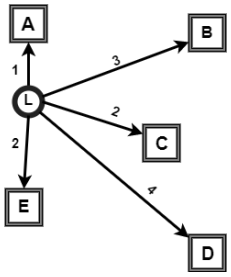

Figure 5.5: RSSI constraints for Node L and anchor points A,B,C,D and E

whose position is to be determined. The signal from L is captured by all the anchor points with different signal strengths. A constraint table is then created based on the received signal from the beacons. Let $R_{N\times N}$ represent the RSSI constraint table from n beacons. Each element can be determined as follows :

$$R_{N\times N}(i,j) = \begin{cases} 1, & \text{If } RSSI_i > RSSI_j \\ 0, & \text{If } RSSI_i = RSSI_j \\ -1, & \text{If } RSSI_i < RSSI_j. \end{cases} \tag{5.11}$$

Another table termed as distance constraint $D_{N\times N}$ is constructed for each point P in the localization space by calculating the distance between the point P and the n beacon nodes.

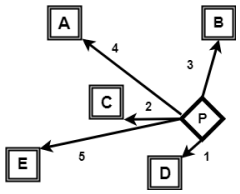

Figure 5.6: Distance constraints constraints for P and anchor points A,B,C,D and E

Figure 5.6 shows the distance constraints for a grid point P and beacon nodes A,BC,D and E. Due to the relationship between RSSI and distance if the reference nodes are ranked in the decreasing order of RSSI then this should ideally represent the increasing order of distance to the unknown node. If R_i and d_i are RSS and distance then:

$$R_i > R_j \Rightarrow d_i < d_j \quad \forall i < j \tag{5.12}$$

Thus distance constraints table $D_{N\times N}$ is determined as

$$D_{N\times N}(i,j) = \begin{cases} 1, & \text{If } d_i < d_j \\ 0, & \text{If } d_i = d_j \\ -1, & \text{If } d_i > d_j \end{cases} \tag{5.13}$$

The tables $R_{N\times N}$ and $D_{N\times N}$ have the same structure and dimension. The localization algorithm compares these two tables and determines the number of constraints that are satisfied and selects the location that maximizes the number of satisfied constraints.

In most cases the assumption in Equation 5.12 holds. However due multipath, reflection and absorption of signals, there might be flips in the sequence i.e $R_i < R_j$ although $d_i > d_j$. However the location can still be estimated if most of the constraints are satisfied. Hence the localization accuracy depends on the amount of noise in the environment.

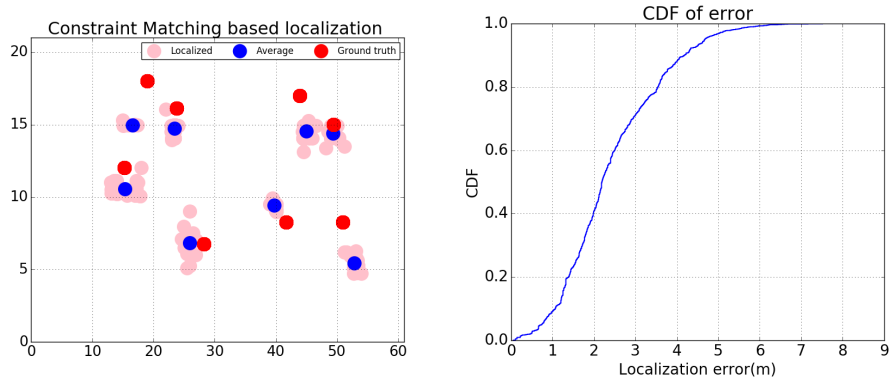

(a) (b)

Figure 5.7: Scatter plot of Localization and CDF of error

Proposal to Improve Position Estimation and Execution Time

The ECL algorithm estimates the position by doing an exhaustive search on all possible points in the localization area. This can be highly time consuming if the area is large with high number of anchor points. In our experiments as testbed is 60m x 20m with more than 50 sniffers acting as anchor points. The algorithm takes large time to give out each position estimate. In order to reduce the computation time we need to perform constraint matching only in selective regions instead of doing it for the complete space.

We propose two methods that were investigated to reduce the execution time:

- Doing a primary constraint matching with lower resolution of points say every 5-10m and find the points with highest scores in order to know the approximate area where the unknown node is located. Do a secondary constraint matching in a more exhaustive manner within the approximated zone.

- Find the approximate zone based on signals from the first S strongest sniffers. Form a bounded polygon based on lowest and highest dimensions of the strongest sniffers. Apply constraint matching within the bounded polygon. Choosing appropriate value of S determines the area of the resulting polygon area. If $(S = N)$ then complete localization space is considered.

The second method is better as it requires performing constraint matching calculations only once. The highlighted part in Figure 5.8 shows the locations where constraint matching is applied. Figure 5.8(a) depicts the naive algorithm which employs exhaustive search irrespective of the position of the unknown node. A lot of time can be saved if we apply constraint matching only within the bounded polygon formed by four strongest sniffers, this is depicted in Figure 5.8(b). Table 5.1 shows the improvement in execution time. Having an approximate pre-localization stage before actual localization can reduce the execution time by almost 8 times.

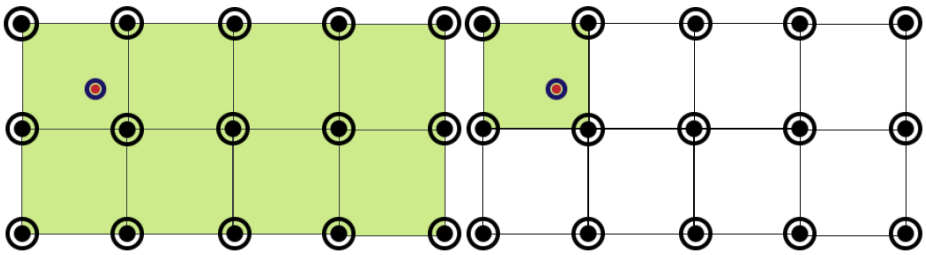

(a) (b)

Figure 5.8: Bounded polygon method to improve position estimation in constraint matching

Algorithm	**Execution time (ms)**
Naive ECL	1200
Modified ECL	168

Table 5.1: Execution times for naive and modified approach

As the number of sniffers reduce, the number of locations with similar constraints increase within the localization space this reduces the localization accuracy. By limiting the area before performing location estimation we can minimize the errors to an extent. Figure 5.9 shows the variation of localization accuracy after significantly reducing the number of sniffers from every 6 m to every 18 m at the testbed. Figure 5.9(a) shows the CDF of errors for the naive algorithm that considers every possible location in the localization space. Figure 5.9(b) shows CDF of errors based on bounded polygon approach.

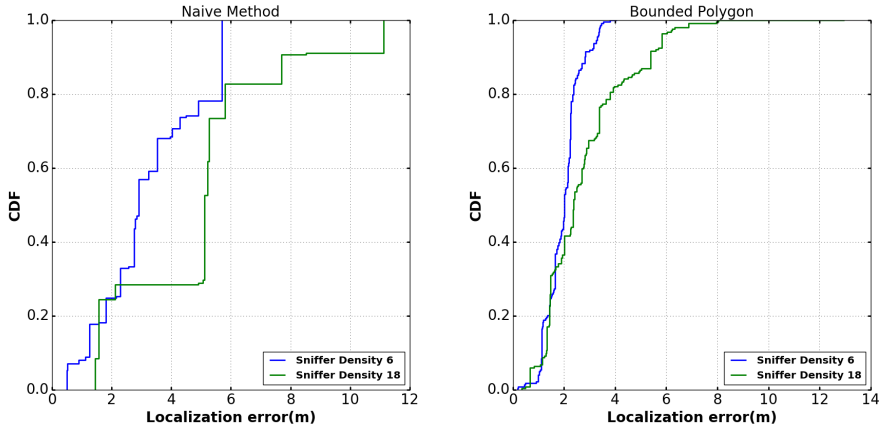

(a) (b)

Figure 5.9: Improvement in position estimation using bounded polygon.

5.4.3 Lateration

Lateration is one of the most widely adopted localization algorithms. It is a simple range based technique based on basic geometric principles. It is based on the idea that if the exact distance to an unknown node can be calculated from at least three known anchor points then the position of the node can be determined by the intersection point of these circles. The method is called trilateration if three anchor points are used or multilateration in case more than three anchor points are used for position estimation.

Lateration involves calculating distances form the anchor points based on received signal strength. Mathematical models are used to correlate an RSSI value to a distance estimate. As RSSI values are prone to error due to multiple factors there will always be noise associated with the measurements hence the circles will not intersect at exactly one point. Thus we make use of several techniques to arrive at the closest possible solution.

Let $P(x, y)$ be the position of the unknown node. Let d_i be the distance estimated from anchor node P_i whose location (x_i, y_i) is known in advance. The distance d_i between these points can be expressed with distance formula as:

$$d_i = \sqrt{(x - x_i)^2 + (y - y_i)^2} \tag{5.14}$$

Taking square on both sides:

$$\begin{aligned} d_i^2 &= (x - x_i)^2 + (y - y_i)^2 \\ &= x^2 - 2xx_i + x_i^2 + y^2 - 2yy_i + y_i^2 \end{aligned} \tag{5.15}$$

In order to eliminate the non-linear terms x^2 and y^2 we subtract d_N^2 from d_i^2 resulting in $N - 1$ equations.

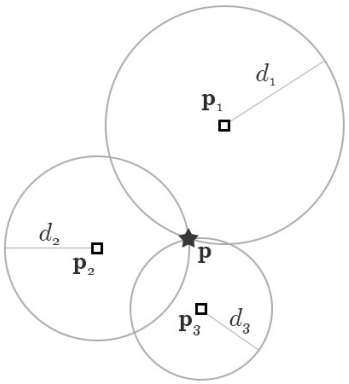

Figure 5.10: Estimating the position of an unknown node by trilateration

$$\begin{aligned} d_i^2 - d_N^2 &= x^2 - 2xx_i + x_i^2 + y^2 - 2yy_i + y_i^2 - (x^2 - 2xx_N + x_N^2 + y^2 - 2yy_N + y_N^2) \\ &= -2x(x_i - x_N) + x_i^2 - x_N^2 - 2y(y_i - y_N) + y_i^2 - y_N^2 \end{aligned} \tag{5.16}$$

Equation 5.16 after reordering can be expressed in matrix form as :

$$\mathbf{b} = \mathbf{A}\,[x\ y]^T \tag{5.17}$$

where:

$$\mathbf{b} = \begin{bmatrix} d_1^2 - x_1^2 - y_1^2 - d_N^2 + x_N^2 + y_N^2 \\ d_2^2 - x_2^2 - y_2^2 - d_N^2 + x_N^2 + y_N^2 \\ \vdots \\ d_{N-1}^2 - x_{N-1}^2 - y_{N-1}^2 - d_N^2 + x_N^2 + y_N^2 \end{bmatrix}$$

$$\mathbf{A} = -2 \begin{bmatrix} x_1 - x_N & y_1 - y_N \\ x_2 - x_N & y_2 - y_N \\ \vdots & \vdots \\ x_{N-1} - x_N & x_{N-1} - x_N \end{bmatrix}$$

Equation 5.17 can be solved using linear least squares approach:

$$\mathbf{P}(\mathbf{x}, \mathbf{y}) = (\mathbf{A}^\top \mathbf{A})^{-1} \mathbf{A}^\top \mathbf{b} \tag{5.18}$$

In some cases the inverse of matrix cannot be calculated due to which the lateration might fail. In order to avoid this, we also explore non-linear least sqaures approximation method. The multilateration problem can be seen as an optimization problem where we try to minimize the sum of squares of the errors on the distance. If $\hat{d}_i$ represents the exact distance between the unknown node and the i^{th} anchor point and d_i represents the approximate estimated distance. Then $\hat{d}_i$ can be represented as:

$$(x - x_i)^2 + (y - y_i)^2 = \hat{d}_i^{\,2} \tag{5.19}$$

In order to find the closest position we must try to minimize the function:

$$F(x,y) = \sum_{i=1}^{n} (\hat{d}_i - d_i)^2 = \sum_{i=1}^{n} \left(\sqrt{(x-x_i)^2 + (y-y_i)^2} - d_i \right)^2 \tag{5.20}$$

Many mathematical algorithms are available to minimize the sum of squares. In our approach we chose Levenberg–Marquardt algorithm [27] to solve the non-linear least squares problem.

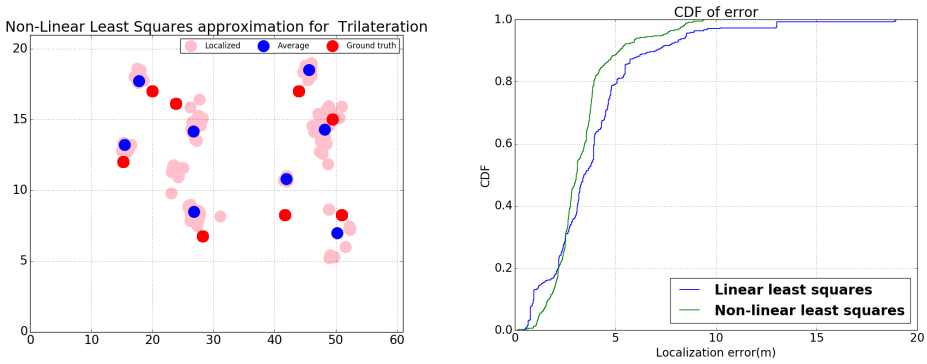

(a) (b)

Figure 5.11: Scatter plot for localization along and CDF of error

Figure 5.11 shows the scatter plot and CDF of error for both Linear and Non-Linear least squares approximation. It was observed that Linear Least Squares method failed multiple times as suspected. The performance of Non-Linear Least Squares approximation methods was found to be much better with 80% of the predicted values within 5 m. However the main drawback of both these methods is that they require efficient estimation of path loss exponent (γ) and received power at a reference distance in order to calculate distance. If these parameters are not estimated properly errors are introduced in distance estimation which leads to inaccurate position estimation.

5.5 Comparison

In this section we provide a comparative analysis of the localization algorithms explained previously with respect to various parameters in order to understand their performance.

5.5.1 Number of samples

Due to the nature of smartphones, getting a high number of samples is not always guaranteed. Therefore the localization algorithm should be able to

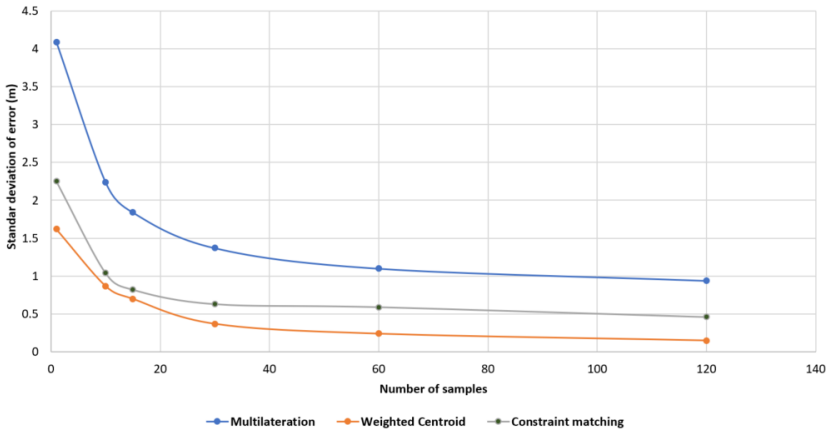

Figure 5.12: Comparison of standard deviation of error for different number of samples

provide a decent accuracy even with less samples.

From Figure 5.12, it can be seen that multilateration performs significantly worse under lower sample sizes compared to the other two algorithms. This can be attributed to that fact that multilateration is a range based algorithm and position estimation errors occur due to errors in distance estimation as a consequence of high RSSI variance.

5.5.2 Sniffer Density and Topology

This parameter refers to the performance of localization algorithms with respect to number sniffers deployed in the area and topology of deployment. Sniffer density refers to the distance between adjacent sniffers for a given topology. Simulations were run with different sniffer densities for two basic types of topologies namely square and diamond. The detailed description of simulations is in chapter 6. The detailed Figure 5.13 shows the maximum error noticed in simulations under different sniffer densities.

Diamond topology of deployment performs better as every point within the localization space will be covered by at least 3 sniffers. More on coverage is explained in Chapter 6 Section 6.2. Although the maximum error observed decreases with the number of beacon nodes, Weighted Centroid and Constraint matching clearly perform better than Multilateration even at lower sniffer densities irrespective of the topology of deployment.

5.5.3 Execution Time

The time required to calculate a single position estimate is calculated for all the localization algorithms. The time is calculated for a set of 30 samples

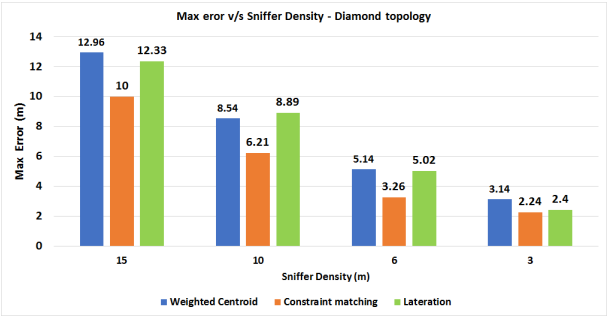

(a)

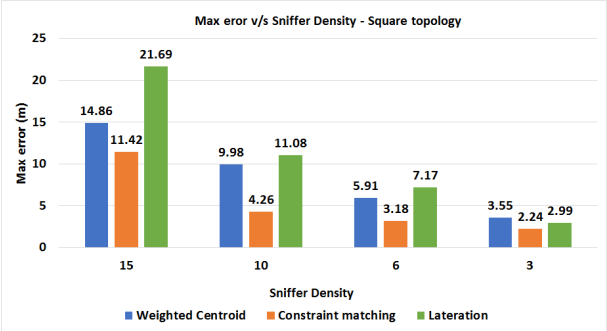

(b)

Figure 5.13: Variation of maximum error in simulations for different sniffer densities

from the testbed data where the sniffer density is every 6m in a square deployment pattern.

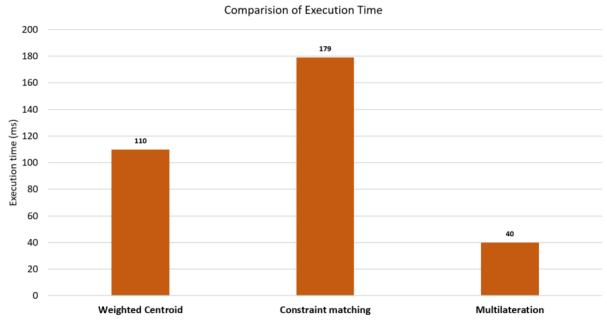

Figure 5.14: Comparison of execution time for different localization algorithms.

As seen in Figure 5.14, constraint matching algorithm takes more time compared to all the algorithms. This is because constraint matching compares the sequences for a number of points within the localization space in

order to make the position estimation. Multilateration consumes the least time as it is computationally less intensive compared to the other methods.

5.6 Confidence Scores

The problem of localizing an individual based on sparse signals from the smartphone with all the given constraints is a difficult task. It was aptly described by one of the supervisors as synonymous to "Finding a black cat in a dark room". Hence we try to associate confidence scores with each localization prediction. Confidence scores give us an idea about the reliability of a specific prediction. To generate a score we take into account the following metrics.

- RSSI Variance: Multipath, reflection and absorption of radio signals can introduce a lot of noise into the signals which increases the variance in RSSI samples. Higher RSSI variance leads to unstable prediction of location.

- Number of Samples (η): We can combat the effect of RSSI variance by applying appropriate filtering and smoothing techniques. However we need sufficiently higher number of samples to perform effective filtering and smoothing. Thus higher number of samples can lead to good prediction. This may not always be guaranteed and depends on the configuration of the smartphone.

- Polygon area: This factor is dependent on the topology of sniffers in the localization space. It refers to the area of polygon formed by the S strongest sniffers. For instance if the deployment is in the form of a diamond grid. Any point falls within one of the triangles. If $n = 3$ then three strongest sniffers should ideally form a triangle as shown in the figure. However due to several factors such as one of the sniffers loosing a packet or due to RSSI variance the four strongest sniffers might deviate from the ideal location which can be an indication of poor localization prediction.

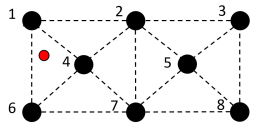

Figure 5.15: Polygon area for predicting localization accuracy

In Figure 5.15, ideally he three strongest sniffers should be 1,4 and 6. In case sniffer 4 fails to capture the signal, the three strongest sniffers will be either $\triangle 126$ or $\triangle 127$ whose area is much larger than

Metric	Scoring Rubrics							
	Poor		Moderate		Good		Best	
Number of Samples (N)	Value	Score	Value	Score	Value	Score	Value	Score
	<5	0.1	[5,15]	0.35	[15,30]	0.75	>=30	1
Polygon Area(A)	<12.5 or >75	0.2	[50,75]	0.35	[24.5,50]	0.75	[12.5,24.5]	1
Variance (V)	>1	0.2	[0.75 ,1]	0.5	[0.25, 0.5]	0.75	<=0.25	1

Table 5.2: Detailed rubrics for confidence score generation

Sl.No	**Score**	**Estimation Error (m)**	**Variance**	**Polygon Area**	**Samples**
1	70.5	3.10	0.47	43	7
2	52.5	3.761	0.58	43	2
3	89.5	2	0.68	21	47
4	95.5	0.94	0.48	21	56

Table 5.3: Confidence scores based on RSSI Variance, Number of Samples and Polygon area

△146. In our experiments at the testbed minimum horizontal and vertical distance between sniffers is $7m$ and $3.5m$ respectively. Thus an elemental square block would be $24.5m^2$ if farther way sniffers are used for localization this area increases which also has impact on localization accuracy.

The number of samples (η), RSSI Variance (V) and the polygon area (A) are categorized into various bins and score is associated depending on their deviation from the ideal values. The total score out of hundred can be calculated as

$$\text{Score} = (0.4A + 0.3\eta + 0.3V)\,100 \tag{5.21}$$

It should be noted that the scores only provide an indication of how reliable a specific estimation can be, a high score can indicate good localization accuracy whereas an estimate with low error may end up having a bad score. The detailed scoring rules are shown in Table 5.2. The values for choosing a specific category (Good,poor,moderate, best) are based on experimental results from the testbed. From Equation 5.21, it can be seen that more weight (40%) is given to polygon area and the rest is divided between RSSI variance and the number of samples as polygon area is better indicator of accuracy. Table 5.3 indicates scores generated for some localization estimates.

The results of the localization experiments at the testbed and simulations indicate that range free localization algorithms such as WCL and CM perform better than Multilateration. Confidence scores give us a metric to filter out estimates that may be unreliable.

Chapter 6

Optimal Grid Configuration

This chapter provides an overview of a favourable sniffer deployment strategies. Section 6.2 describes the problem of area coverage in detail and describes algorithms that can be used to verify the coverage within a given area. Section 6.3 explains optimal deployment of sniffers, an ILP is formulated to describe deployment of sniffers such that every point in the localization space is covered by a certain number of sniffers. Simulations are used to minimize the number while maintaining a required accuracy.

6.1 Introduction

Since Wi-Fi sniffers are placed as part of the lighting infrastructure, it is important to understand how localization schemes might perform under different lighting grid topologies and sniffer densities. Although it is trivial that the localization accuracy increases with increase in density of anchors points, we need to find a sweet spot where we can expect a decent localization accuracy with a reasonable density of sniffers. This parameter has a direct impact on the deployment cost of the system as bulbs with sniffers cost more than the regular ones.

6.2 Sensor Area Coverage

Sensor area coverage is one of the most important performance parameters we need to keep in mind as it reflects how well a target area is covered by the deployed sniffers. Achieving sufficient coverage in the region of interest while minimizing the number of sniffers can be a challenging task. Coverage can have direct impact on localization algorithms as many algorithms require minimum 3-4 sniffers in the area for a good localization accuracy. The coverage problem is very popular in many research fields. The Art Gallery problem [30] is a popular area coverage problem which tries to minimize the

number of observers required to monitor a polygon area. For our application the k coverage problem can be split into two subsections.

- Verification : Check if all the points within the localization space are within the coverage area of at least k sniffers.
- Selection : Minimize the number of sniffers while ensuring k-coverage in the area. This is done by selecting a subset of sniffers under the assumption that a sniffer is present uniformly every n meters.

Problem Definition : Let $S = \{s_1, s_2, ...s_N\}$ denote the set of all the sniffers and $P = \{p_1, p_2, ...p_M\}$ denote the set of all locations in the deployment area. The sensing range of each sniffer $s_i \in S$ can be represented by a circle of radius r_i. A point p_i is said to be within the sniffing range of s_i if the distance d_i between center of circle s_i and point p_i is less than the radius r_i. We need to determine if all the points in the deployment area P are within the sensing range of at least k sniffers where $k \geq 3$.

The coverage problem has been previously addressed by many researchers. So et al. [34] proposed the use of Voronoi diagrams to identify the worst case and best case coverage areas in a given space. The algorithm tries to to find paths between an initial and final location so as to include regions which are not covered by k sensors. In order to address the area coverage we adopt the work from Huang et al. [23] as its more aligned with our application.

The k coverage is verified by checking if the perimeter of each sniffer is k-covered. It has been proven that entire region is k-covered if all the points on the perimeter are k-covered. The distance between the centers are calculated to first verify if they intersect. Sniffers s_i and s_j intersect each other if the distance between their centers d is less than $2r$.

$$d_{ij} = \sqrt{(x_i - x_j)^2 + (y_i - y_j)^2} \leq 2r \tag{6.1}$$

For each sniffer s_i amount of overlap with its neighbouring sniffer s_j is determined by calculating the perimeter of s_i in s_j. From Figure 6.1, we can see that the angle α can be obtained using trigonometric properties as $\alpha = cos^{-1}\left[\frac{d_{ij}}{2r}\right]$.

The perimeter of s_i falling within the range $[\pi-\alpha, \pi+\alpha]$ inside s_j is said to be perimeter covered by s_j. The start and end of such segments are denoted as $[\alpha_{jL}, \alpha_{jR}]$. Such points are calculated for all the neighbouring sniffers of s_i and placed on a line segment $[0, 2\pi]$. The points are then sorted in an ascending order into a list L. The perimeter coverage of s_i is then determined by traversing the line segment from left to right while visiting each element. This is illustrated in Figure 6.1. The cost of the algorithm is $O(nd \log d)$ where d is the maximum number of neighboring sniffers for a given sniffer. Thus given a configuration of sniffers we can determine if each point in the area is covered by at least 3-4 sniffers.

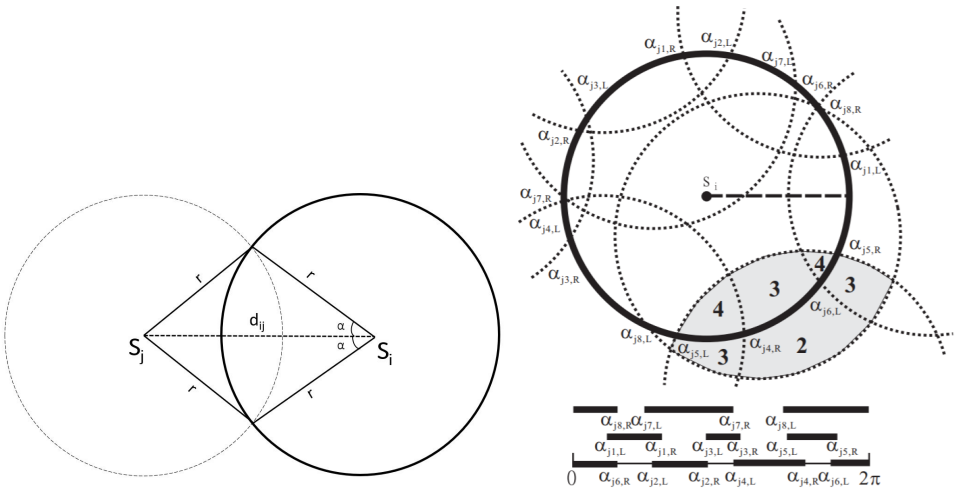

(a) (b)

Figure 6.1: Perimeter coverage of S_i by traversing the line $[0, 2\pi]$ as mentioned in [22]

Figure 6.2 shows the difference in coverage between square and diamond deployment. Square topology shows coverage holes where as every point diamond deployment is covered.

6.3 Optimal Sniffer Deployment

This k-coverage problem has been proved to be NP-complete by reduction to the minimum dominating set problem by Patterson et al. [47]. The problem of minimizing the number of sniffers while maintaining k-coverage can also be approximated using an ILP formulation. The localization space can be considered as bounded region with n discrete points arranged as a grid. As mentioned previously each sniffer has an effective sensing range of r. For simplicity its assumed that all the sniffers have uniform range. Each point in the localization space can be occupied by at most one sniffer. We need to minimize the number of sniffers such that each point is within range of at least k sniffers ($k \geq 1$). This problem can be formulated as an Integer Linear Program (ILP).

ILP Formulation

Let d_{ij} denote the Eucledian distance between two points i and j. Let E_v denote set of points such that distance between them d_{ij} is within the sensing

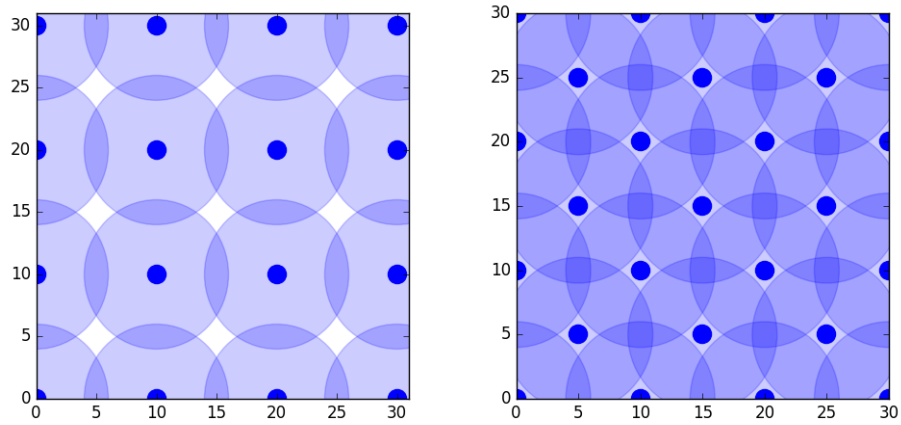

(a) (b)

Figure 6.2: Coverage shown by overlapping circles for square and diamond deployments

range r of sniffers.

$$E_v = \{(i,j)|0 \leq d_{ij} < r\}$$
$$E_v[i] = \{j|(i,j) \in E_v\}, i = 1,2,3,...,n$$

Let C be the deployment cost of the sniffer. Let x_i be a variable to denote if a sensor is already placed at point i.

$$x_i = \begin{cases} 1, & \text{If sensor is placed at point i} \\ 0, & \text{otherwise} \end{cases}$$

We need to minimize the cost of sniffers :

$$\text{Min} \sum_{i=1}^{n} C \cdot x_i \tag{6.2}$$

such that :

$$\sum_{j \in E_v[i]} x_j \geq k \ \forall i \tag{6.3}$$

Constraint 6.3 ensures that the points are covered by at least k sniffers.

As k-coverage is an NP-complete problem, solving the ILP formulation given by Equation 6.2 involves checking constraints for every possible combination of sniffer locations within the given dimensions. However as sniffers are part of a lighting grid some of the constraints become relaxed.

- Fixed Sniffer topology i.e, locations that a sniffer can be installed is predefined.

- Minimum separation between sniffers need to be maintained depending on the sniffer density.
- As wireless signals degrade with increasing distance we can establish a maximum bound between sniffers beyond which localization accuracy drops significantly

Therefore we do not use any heuristics to solve the formulated ILP. Instead we perform simulations for different topologies and distribution of nodes under varying levels of sniffer densities.

Simulations provide us more freedom to vary parameters such as location of sniffers and distribution of nodes. As the testbed is quite large and there are limited number of robots its difficult to understand how the accuracy of localization varies for different regions in the localization space.

In simulations we can spread the unknown nodes either randomly in the localization space or uniformly at each point. This can give us an idea about the maximum error that can be expected. Mainly two topologies are considered due to their popularity and usage. The topologies along with possible choices for node distribution are as shown in Figure 6.3. Figure 6.3(a) shows square pattern of sniffers with randomly distributed nodes in the area where as Figure 6.3(b) shows diamond pattern with uniformly distributed nodes, other variants of topology can be derived using these basic types.

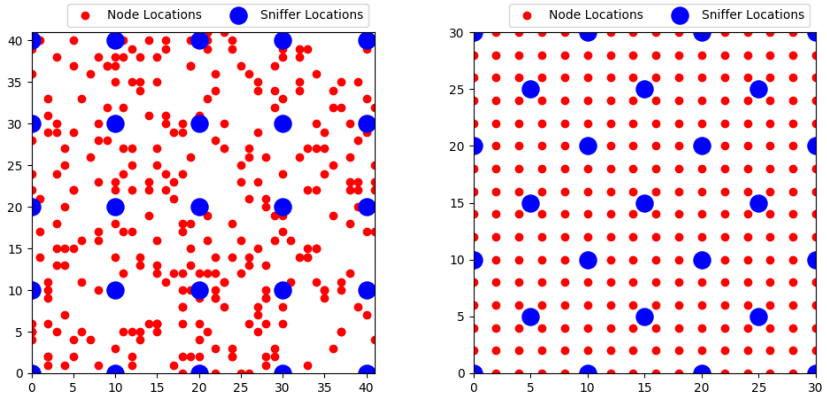

(a) (b)

Figure 6.3: Square topology with randomly distributed nodes and Diamond topology with uniform node distribution

Simulations are performed on a 30m x 30m grid where the sniffer density is varied from 4m to 15m. In random configuration 100 nodes are placed on random locations within the grid. In uniform configuration a node is placed

every 2 meters in both horizontal and vertical dimensions. Log normal shadowing model is used to generate RSSI values with path loss exponent γ= 1.3. Noise is introduced into the simulations by adding random error with zero mean and a standard deviation of 1 is to the RSSI values. In order

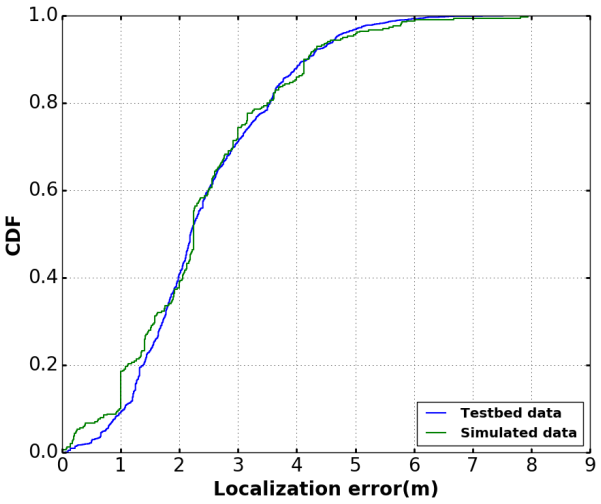

Figure 6.4: Comparison of CDF of error for simulation and testbed data

to validate simulations we recreated the topology from the testbed and the output from simulations were compared with the data from testbed. Figure 6.4 shows the similarity between simulation data and the data taken from the tesbed.

Figure 6.6 and 6.7 show the results of the simulations for diamond and square topology of deployment with different sniffer densities. Simulations indicate that range free localization algorithms with diamond deployment perform better.

Sniffer Density	**Accuracy <2m**	**Accuracy <2.5m**
3	80%	95%
4	74%	82%
5	52%	70%
6	55%	55%

Table 6.1: Sniffer densities and associated localization accuracy

Figure 6.5(a) and (b) shows the result of simulations for a topology similar to the testbed (61m x 21m) using CM and WCL respectively. The results are summarized in table 6.1. Although 3m can be considered as the most optimum one where 80% of values are within 2m, we can save lot of bulbs if

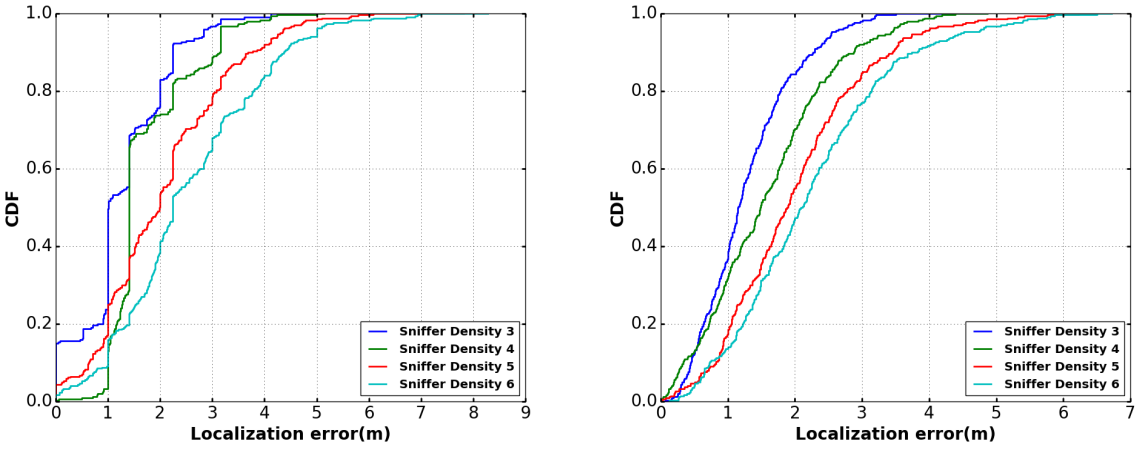

(a) (b)

Figure 6.5: Simulation results for testbed topology

we deploy a sniffer every 4m which provides estimates close to 70% of time $\leq$ 2m and 2.5m $\geq$80% of time.

Figure 6.6 shows CDF of errors for diamond topology with different localization algorithms for 30mx30m grids. Figure 6.7 shows CDF of errors for square topology for same scenario. It can be range free localization algorithms provide better results even when the sniffer density is low.

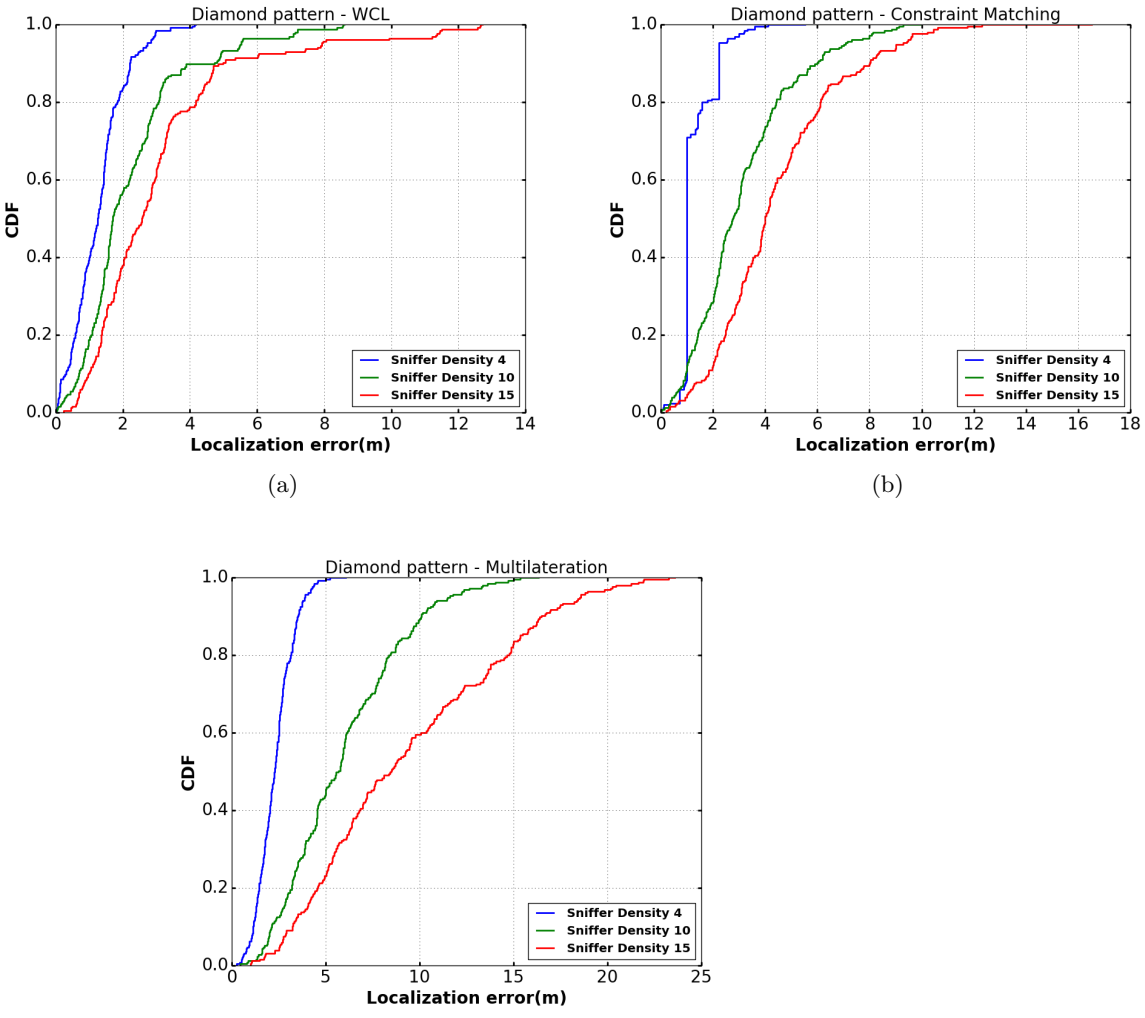

Figure 6.6: CDF of errors for different localization algorithms and sniffer densities for diamond topology

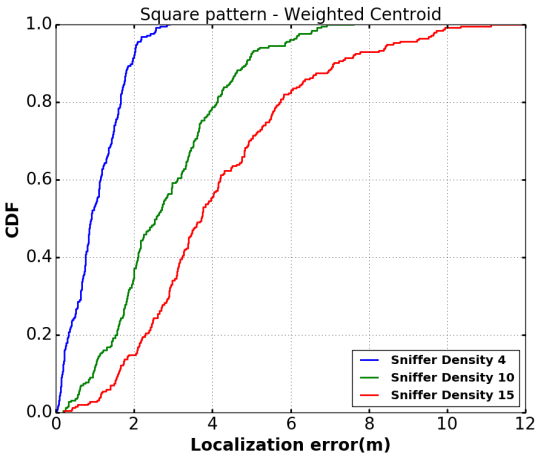

(a)

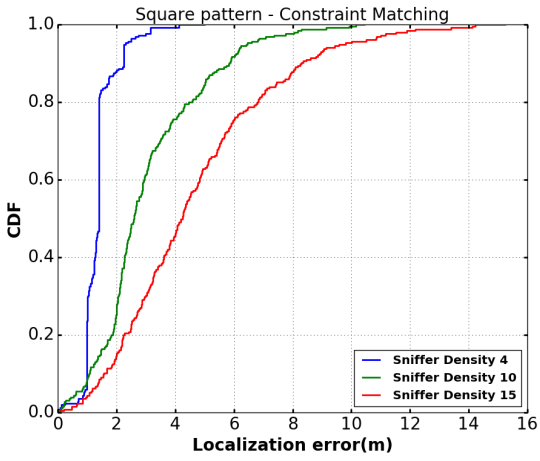

(b)

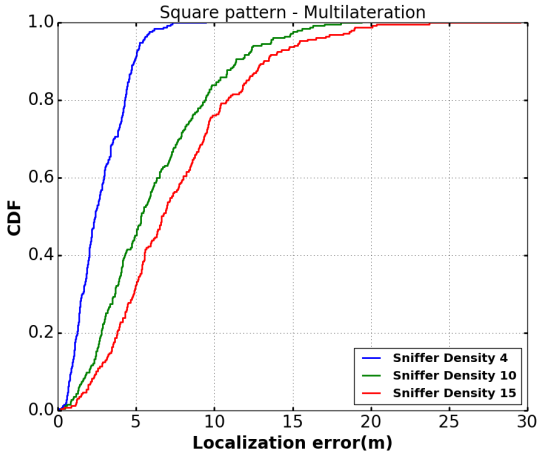

(c)

Figure 6.7: CDF of errors for different localization algorithms and sniffer densities for square topology

Chapter 7

Conclusions and Future Work

7.1 Conclusions

In this thesis the feasibility of using Wi-Fi sniffing to infer the crowd distribution in a given area was studied. The idea was to incorporate Wi-Fi sniffing into smart light bulbs as part of the lighting grids in order to measure number of people in a given area and approximate spatial distribution by sniffing for smartphones that people might carry with them. It is assumed that most of the people carry smartphones with them and have their Wi-Fi turned on. As Wi-Fi sniffing is non-intrusive we do not possess any control over how a specific smartphone sends packets. Thus, the problem on hand was interesting as well as extremely challenging.

First, sniffing experiments were conducted in order to analyze the time resolution and diversity of packets under different smartphone configurations. The data from CRAWDAD repository containing traces from over 3000 smartphones was also analyzed. Experiments indicate that although the time interval between packets radically differs depending on the configuration. On the average, packets can be seen within 60 seconds from most of the phones. When Wi-Fi data is used, a packet can be seen almost every second which can be considered as the best case scenario with worst case interval being 3-5 minutes. This indicates that a system can be designed with a minimum sampling interval of 30-60 seconds. Any value lower than this will increase the false positives in the system.

The data from multiple sniffers deployed in an area is aggregated to count the number of people. Several filtering and post processing mechanisms were proposed in order to eliminate noise and false positives due to unwanted devices encountered during sniffing. Experiments to count the number of people were conducted under controlled conditions with a Wi-Fi testbed and also in a live test setup (auditorium,coffee corner). Each of these scenarios

represents a different type of crowd setting. The DoVo room represents a scenario where people hardly move during the course of the event. Whereas coffee corner represents a more dynamic environment where people can engage in conversations and spend lot of time or quickly grab coffee and move. The counting algorithm was evaluated against the ground truth either by manual counting or by the use of cameras. Results indicate that counting algorithms came close to 75% of the ground truth for the DoVo room.

Due to the imposed constraints on the system RSSI based localization schemes were used to infer spatial distribution of devices in the given area. Experiments were conducted at a testbed to evaluate different localization algorithms. Mobile robots with Wi-Fi interface were used to mimic movement of people. Three different localization schemes namely Weighted Centroid (WC), Multilateration (ML) and Constraint Matching (CM) were evaluated to analyze their feasibility of usage. Localization results indicate that range free localization schemes such as WC and CM perform much better compared to ML. ML suffers as it requires estimation of the distance based on path loss models, even Small errors in distance estimation introduces errors in position estimates. Simulations indicate that although 3m can be considered as ideal deployment which gives results within 2m $\geq$ 80% of the time. A deployment 4m can be considered more ideal as we still get an accuracy of $\leq$ 2m 76% of the time.

As localization can be unreliable due to several uncontrollable parameters a confidence score was proposed to assess the reliability of a specific position estimate. It is a weighted score that takes into account several factors such as variance of RSSI values, number of samples used for prediction and the polygon area formed by sniffers having the highest RSSI values. The scoring mechanism is not a measure of localization accuracy but a measure of conditions in which a specific prediction happened. Having this information can help us in filtering out predictions that might be unreliable.

7.2 Future Work

Some of the directions for future research are summarized as follows

- The accuracy of people counting by Wi-Fi sniffing can be influenced by several factors such as the demography of the crowd as explained in section 4.6. A future research direction should take into account certain heuristics and statistics of smartphone usage among different age groups in order to further refine the count based on these properties.

- Due to the growing adoption of the 5GHz band most of the devices can easily switch between 2.4GHz and 5GHz bands. Hence the hardware should also be capable of sniffing on both the bands. The current hardware used for sniffing does not support this. Sniffing data simul-

taneously on both bands and aggregating the this data should further improve the counting performance.

- Analyzing social interactions among the people in the crowd is another interesting area of research. The remembered SSID information in the sniffed probe request frames can be used an input to analyze social interactions.

- The current solutions for crowd distribution analysis uses commercially available off the shelf hardware. A more sophisticated hardware can reveal information that can be used to refine position estimation.

Bibliography

[1] Ieee standard for information technology–telecommunications and information exchange between systems local and metropolitan area networks–specific requirements part 11: Wireless lan medium access control (mac) and physical layer (phy) specifications. *IEEE Std 802.11-2012 (Revision of IEEE Std 802.11-2007)*, pages 1–2793, March 2012.

[2] Naeim Abedi, Ashish Bhaskar, and Edward Chung. Bluetooth and wi-fi mac address based crowd data collection and monitoring: Benefits, challenges and enhancement. In *Australasian Transport Research Forum, ATRF 2013 - Proceedings*, 10 2013.

[3] Utku Gunay Acer, Geert Vanderhulst, Afra Masshadi, Aidan Boran, Claudio Forlivesi, Philipp M Scholl, and Fahim Kawsar. Capturing personal and crowd behavior with wi-fi analytics. In *Proceedings of the 3rd International on Workshop on Physical Analytics*, pages 43–48. ACM, 2016.

[4] Fadel Adib and Dina Katabi. See through walls with wifi! *SIGCOMM Comput. Commun. Rev.*, 43(4), Aug. 2013.

[5] Marco V Barbera, Alessandro Epasto, Alessandro Mei, Vasile C Perta, and Julinda Stefa. Signals from the crowd: uncovering social relationships through smartphone probes. In *Proceedings of the 2013 conference on Internet measurement conference*, pages 265–276. ACM, 2013.

[6] Jan Blumenthal, Ralf Grossmann, Frank Golatowski, and Dirk Timmermann. Weighted centroid localization in zigbee-based sensor networks. In *Intelligent Signal Processing, 2007. WISP 2007. IEEE International Symposium on*, pages 1–6. IEEE, 2007.

[7] B. Bonn, A. Barzan, P. Quax, and W. Lamotte. Wifipi: Involuntary tracking of visitors at mass events. In *2013 IEEE 14th International Symposium on "A World of Wireless, Mobile and Multimedia Networks" (WoWMoM)*, June 2013.

[8] Stefan Bouckaert, Wim Vandenberghe, Bart Jooris, Ingrid Moerman, and Piet Demeester. The w-ilab.t testbed. In *TRIDENTCOM*, 2010.

[9] G. J. Brostow and R. Cipolla. Unsupervised bayesian detection of independent motion in crowds. In *2006 IEEE Computer Society Conference on Computer Vision and Pattern Recognition (CVPR'06)*, volume 1, pages 594–601, June 2006.

[10] N. Bulusu, J. Heidemann, and D. Estrin. Gps-less low-cost outdoor localization for very small devices. *IEEE Personal Communications*, Oct 2000.

[11] Marco Cattani, Ioannis Protonotarios, Claudio Martella, Joost van Velzen, Marco Zuniga, and Koen Langendoen. An open-space museum as a testbed for popularity monitoring in real-world settings. In *Int.\Conf.\on Embedded*

Wireless Systems and Networks (EWSN), volume 8354, pages 265–276. ACM, 2016.

[12] N. Cheng, P. Mohapatra, M. Cunche, M. A. Kaafar, R. Boreli, and S. Krishnamurthy. Inferring user relationship from hidden information in wlans. In *MILCOM 2012 - 2012 IEEE Military Communications Conference*, Oct 2012.

[13] M. Cunche, Mohamed Ali Kaafar, and R. Boreli. I know who you will meet this evening! linking wireless devices using wi-fi probe requests. In *2012 IEEE International Symposium on a World of Wireless, Mobile and Multimedia Networks (WoWMoM)*, June 2012.

[14] B. K. Dan, Y. S. Kim, Suryanto, J. Y. Jung, and S. J. Ko. Robust people counting system based on sensor fusion. *IEEE Transactions on Consumer Electronics*, August 2012.

[15] Saandeep Depatla, Arjun Muralidharan, and Yasamin Mostofi. Occupancy Estimation Using Only WiFi Power Measurements. *IEEE Journal on Selected Areas in Communications*, 2015.

[16] S. Di Domenico, G. Pecoraro, E. Cianca, and M. De Sanctis. Trained-once device-free crowd counting and occupancy estimation using wifi: A doppler spectrum based approach. In *2016 IEEE 12th International Conference on Wireless and Mobile Computing, Networking and Communications (WiMob)*, Oct 2016.

[17] S. H. Doong. Spectral human flow counting with rssi in wireless sensor networks. In *2016 International Conference on Distributed Computing in Sensor Systems (DCOSS)*, May 2016.

[18] Daniel Halperin, Wenjun Hu, Anmol Sheth, and David Wetherall. Tool release: Gathering 802.11n traces with channel state information. *SIGCOMM Comput. Commun. Rev.*, 41(1), Jan. 2011.

[19] Marcus Handte, Muhammad Umer Iqbal, Stephan Wagner, Wolfgang Apolinarski, Pedro José Marrón, Eva Maria Muñoz Navarro, Santiago Martinez, Sara Izquierdo Barthelemy, and Mario González Fernández. Crowd density estimation for public transport vehicles. In *EDBT/ICDT Workshops*, 2014.

[20] Jorge Herrera and Hyung Suk Kim. Ping-pong: Using smartphones to measure distances and relative positions. In *Proceedings of Meetings on Acoustics 166ASA*. ASA, 2013.

[21] Federal Communications Commission http://www.fcc.gov.

[22] Chi-Fu Huang and Yu-Chee Tseng. The coverage problem in a wireless sensor network. In *Proceedings of the 2Nd ACM International Conference on Wireless Sensor Networks and Applications*, WSNA '03, pages 115–121, New York, NY, USA, 2003. ACM.

[23] Chi-Fu Huang, Yu-Chee Tseng, and Li-Chu Lo. The coverage problem in three-dimensional wireless sensor networks. In *Global Telecommunications Conference, 2004. GLOBECOM '04. IEEE*, volume 5, pages 3182–3186 Vol.5, Nov 2004.

[24] IEEE. http://standards-oui.ieee.org/oui.txt.

[25] Shuja Jamil, Anas Basalamah, Ahmed Lbath, and Moustafa Youssef. Hybrid participatory sensing for analyzing group dynamics in the largest annual religious gathering. In *Proceedings of the 2015 ACM International Joint Conference on Pervasive and Ubiquitous Computing - UbiComp '15*, pages 547–558, New York, New York, USA, 2015. ACM Press.

[26] David Kotz, Tristan Henderson, Ilya Abyzov, and Jihwang Yeo. CRAWDAD dataset dartmouth/campus (v. 2009-09-09). Downloaded from https://crawdad.org/dartmouth/campus/20090909, Sept. 2009.

[27] Jorge J. Moré. *The Levenberg-Marquardt algorithm: Implementation and theory.* Springer Berlin Heidelberg, Berlin, Heidelberg, 1978.

[28] A. B. M. Musa and Jakob Eriksson. Tracking unmodified smartphones using wi-fi monitors. In *Proceedings of the 10th ACM Conference on Embedded Network Sensor Systems*, SenSys '12. ACM, 2012.

[29] Farid Movahedi Naini, Olivier Dousse, Patrick Thiran, and Martin Vetterli. Opportunistic Sampling for Joint Population Size and Density Estimation. *IEEE Transactions on Mobile Computing*, 14(12):2530–2543, dec 2015.

[30] Joseph O'Rourke. *Art Gallery Theorems and Algorithms.* Oxford University Press, Inc., New York, NY, USA, 1987.

[31] R. P and M. L. Sichitiu. Angle of arrival localization for wireless sensor networks. In *2006 3rd Annual IEEE Communications Society on Sensor and Ad Hoc Communications and Networks*, Sept 2006.

[32] Steve Rackley. *Wireless Networking Technology: From Principles to Successful Implementation.* Newnes, 2007.

[33] J. Rittscher, P. H. Tu, and N. Krahnstoever. Simultaneous estimation of segmentation and shape. In *2005 IEEE Computer Society Conference on Computer Vision and Pattern Recognition (CVPR'05)*, volume 2, pages 486–493 vol. 2, June 2005.

[34] Anthony Man-Cho So and Yinyu Ye. On solving coverage problems in a wireless sensor network using voronoi diagrams. In *Proceedings of the First International Conference on Internet and Network Economics*, WINE'05, pages 584–593, Berlin, Heidelberg, 2005. Springer-Verlag.

[35] Bo Wu Tao Zhao, Ram Nevatia. Segmentation and Tracking of Multiple Humans in Crowded Environments. *IEEE Transactions on Pattern Analysis and Machine Intelligence*, 2008.

[36] Thiago Teixeira, Gershon Dublon, and Andreas Savvides. A survey of human-sensing: Methods for detecting presence, count, location, track, and identity. *ACM Computing Surveys*, 5(1):59–69, 2010.

[37] Deepak Vasisht, Swarun Kumar, and Dina Katabi. Decimeter-level localization with a single wifi access point. In *Proceedings of the 13th Usenix Conference on Networked Systems Design and Implementation*, NSDI'16, pages 165–178, Berkeley, CA, USA, 2016. USENIX Association.

[38] Yan Wang, Jie Yang, Yingying Chen, Hongbo Liu, Marco Gruteser, and Richard P. Martin. Tracking human queues using single-point signal monitoring. In *Proceedings of the 12th Annual International Conference on Mobile Systems, Applications, and Services*, MobiSys '14, 2014.

[39] Jens Weppner and Paul Lukowicz. Bluetooth based collaborative crowd density estimation with mobile phones. In *Pervasive computing and communications (PerCom), 2013 IEEE international conference on*, pages 193–200. IEEE, 2013.

[40] J. Wilson and N. Patwari. Radio tomographic imaging with wireless networks. *IEEE Transactions on Mobile Computing*, May 2010.

[41] Martin Wirz, Tobias Franke, Daniel Roggen, Eve Mitleton-Kelly, Paul Lukowicz, and Gerhard Tröster. Probing crowd density through smartphones in city-scale mass gatherings. *EPJ Data Science*, 2(5), 2013.

[42] W. Xi, J. Zhao, X. Y. Li, K. Zhao, S. Tang, X. Liu, and Z. Jiang. Electronic frog eye: Counting crowd using wifi. In *IEEE INFOCOM 2014 - IEEE Conference on Computer Communications*, April 2014.

[43] C. Xu, B. Firner, R. S. Moore, Y. Zhang, W. Trappe, R. Howard, F. Zhang, and N. An. Scpl: Indoor device-free multi-subject counting and localization using radio signal strength. In *2013 ACM/IEEE International Conference on Information Processing in Sensor Networks (IPSN)*, pages 79–90, April 2013.

[44] C. Xu, B. Firner, Y. Zhang, R. Howard, J. Li, and X. Lin. Improving rf-based device-free passive localization in cluttered indoor environments through probabilistic classification methods. In *2012 ACM/IEEE 11th International Conference on Information Processing in Sensor Networks (IPSN)*, April 2012.

[45] Mohammad Yamin and Yasser Ades. Crowd Management with RFID and Wireless Technologies. In *2009 First International Conference on Networks & Communications*, pages 439–442. IEEE, 2009.

[46] Mohammad Yamin, Masoud Mohammadian, Xu Huang, and Dharmendra Sharma. RFID Technology and Crowded Event Management. In *2008 International Conference on Computational Intelligence for Modelling Control & Automation*, pages 1293–1297. IEEE, 2008.

[47] Shuhui Yang, Fei Dai, Mihaela Cardei, Jie Wu, and Floyd Patterson. On connected multiple point coverage in wireless sensor networks. *International Journal of Wireless Information Networks*, pages 289–301, 2006.

[48] Kiran Yedavalli, Bhaskar Krishnamachari, Sharmila Ravula, and Bhaskar Srinivasan. Ecolocation: a sequence based technique for rf localization in wireless sensor networks. In *IPSN 2005. Fourth International Symposium on Information Processing in Sensor Networks, 2005.*, April 2005.

[49] Moustafa Youssef, Matthew Mah, and Ashok Agrawala. Challenges: Device-free passive localization for wireless environments. In *Proceedings of the 13th Annual ACM International Conference on Mobile Computing and Networking*, MobiCom '07, 2007.

[50] X. Zhang, J. Yan, S. Feng, Z. Lei, D. Yi, and S. Z. Li. Water filling: Unsupervised people counting via vertical kinect sensor. In *2012 IEEE Ninth International Conference on Advanced Video and Signal-Based Surveillance*, Sept 2012.

[51] T. Zhao, R. Nevatia, and B. Wu. Segmentation and tracking of multiple humans in crowded environments. *IEEE Transactions on Pattern Analysis and Machine Intelligence*, July 2008.